Clim Dyn (2014) 43:2963–2984
DOI 10.1007/s00382-013-2036-x

Are atmospheric biases responsible for the tropical Atlantic SST biases in the CNRM-CM5 coupled model?

A. Voldoire · M. Claudon · G. Caniaux · H. Giordani · R. Roehrig

Received: 30 April 2013 / Accepted: 24 December 2013 / Published online: 10 January 2014

Abstract In this study, the CNRM-CM5 model is shown to simulate too warm SSTs in the tropical Atlantic as most state-of-the-art CMIP5 models. The warm bias develops within 1 or 2 months in decadal experiments initialised in January using an observationally derived state. To better quantify the role of the atmospheric biases in initiating this warm SST bias, several sensitivity experiments have been performed. In a first set of experiments, the surface solar net heat flux sent to the ocean model is academically corrected over the southeastern tropical Atlantic Ocean. This correction locally reduces the warm SST bias by more than 50 % with some remote impacts over equatorial regions. In contrast, the solar heat flux correction has locally little impact on the spring cooling. A second set of experiments quantifies the role of surface winds, using a nudging technique. When applied in a narrow equatorial region, the wind correction mainly improves the SST annual cycle amplitude along the Equator. It promotes not only the spring cooling along the Equator in preconditioning the mixed-layer depth but also in the southeastern Atlantic along the African coast. These local and remote effects are attributed to the more realistic representation of the oceanic equatorial circulation, driven by corrected winds. These results are consistent with those reported by Wahl et al. (Clim Dyn 36:891–906, 2011) in a very similar study with the Kiel Climate Model. The solar and wind biases have comparable effects in their study, although the importance of off-equatorial winds is less clear in our study. Diagnosing the wind energy flux provides a physical understanding of the equatorial region. When combining the corrections of both the equatorial wind and the southeastern solar heat flux, no obvious feedback between them is evidenced. The present study also emphasizes the need to consider two time-scales, the annual mean and the seasonal cycle, as well as two regions, the equatorial and the southeastern Atlantic regions, to comprehensively address the Atlantic SST bias. As pointed out in Richter (Clim Dyn, doi:10.1007/s00382-012-1624-5, 2013), the need to improve the atmospheric component of the CNRM-CM model is emphasized, even though strong positive coupling feedbacks are highlighted.

Keywords Tropical Atlantic · Ocean–atmosphere coupling · Climate · GCM · CMIP5

This paper is a contribution to the special issue on tropical Atlantic variability and coupled model climate biases that have been the focus of the recently completed Tropical Atlantic Climate Experiment (TACE), an international CLIVAR program (http://www.clivar.org/organization/atlantic/tace). This special issue is coordinated by William Johns, Peter Brandt, and Ping Chang, representatives of the TACE Observations and TACE Modeling and Synthesis working groups.

A. Voldoire (✉) · M. Claudon · G. Caniaux · H. Giordani · R. Roehrig
CNRM-GAME (Météo-France/CNRS), Toulouse, France
e-mail: aurore.voldoire@meteo.fr

1 Introduction

Many coupled atmosphere–ocean global climate models (GCMs) have been developed during the last two decades and their realism has greatly improved in the mean time. One of the great challenges of GCM development lies in the realism of the simulated coupled features of the climate system. For instance, in the 90's, climate modellers focussed on the representation of El Niño Southern Oscillation (ENSO), the main mode of tropical variability (IPCC 2007). To improve the representation of ENSO, modellers had to better understand the phenomenon and conversely, models were useful tools to increase our understanding of this coupled feature (Guilyardi et al. 2012). In the recent 5th phase of the coupled model intercomparison project (CMIP5, Taylor et al. 2012), most of state-of-the-art models are able to reproduce the main characteristics of ENSO (Zhang and Jin 2012). In the tropical Atlantic, CMIP5 models are much less realistic (Richter et al. 2012; Toniazzo 2013). There, most of the models simulate a warm bias at the Equator and along the Angola/Namibia coast. The main mode of inter-annual variability in the tropical Atlantic (Atlantic Niño, Zebiac 1993), which mainly corresponds to an amplification of the seasonal cycle, is also rarely properly simulated in GCMs (Joly and Voldoire 2010; Richter 2013).

In these models, the sea surface temperature (SST) bias impacts on the simulation of the low-level atmospheric circulation and thus on the West African monsoon precipitation. The meridional surface temperature gradient is underestimated, so that monsoon precipitation is shifted southward compared to observations in many CMIP5 models (Roehrig 2013). Additionally, as models do not capture the observed Atlantic Niño mode, their ability to reproduce the observed interannual variability of precipitation in the region is limited. This, in turn, limits their ability to provide useful seasonal forecasts over the region (Batté and Déqué, 2011). Climate projections of African monsoon precipitation at the end of the XXIst century are also very uncertain (IPCC 2007; Roehrig 2013). To improve our confidence in climate models over this region, there is thus a need to tackle directly their mean SST biases in the tropical Atlantic.

The equatorial Atlantic SST bias manifests itself as a reversed thermocline east–west gradient simulated in the models (Richter and Xie 2008). Many authors pointed out the role of atmospheric wind biases as a driver of the erroneous ocean mean state (Wahl et al. 2011; Chang et al. 2007). The SST bias along the African coast is also often attributed to atmospheric radiative biases due to the difficulty of atmospheric models to simulate the low level atmospheric humidity and the strato-cumulus cloud cover over this region (Hu et al. 2011). Lin (2007) also showed that the sensitivity of stratus clouds to SST is too weak in CMIP3 models, reinforcing the SST bias. Other studies emphasize the role of ocean models which do not properly simulate the coastal upwelling. The warm bias in the southeastern tropical Atlantic is similar to the bias found in the southeastern tropical Pacific. CMIP3 models suffer from insufficient coastal upwelling along the Peruvian coast as well as too weak Ekman currents that do not properly advect cold water offshore (Zheng et al. 2011). These drawbacks are often attributed to the insufficient horizontal resolution of the oceanic models (Zheng et al. 2011; Seo et al. 2006). Similarly, based on local buoy observations, deSzoeke et al. (2010) showed that the surface solar heat flux is over-estimated by models in the region but also that the ocean cooling is underestimated by the ocean component.

To better quantify the role of these different processes in setting the warm SST bias, the primer idea would be to assess the ability of the atmospheric and oceanic components separately. However, forced ocean simulations are generally driven by near surface temperature and thus the representation of SSTs is nearly driven by the forcing. As noted by Lubbeke et al. (2010), forced ocean simulations using bulk formulae are of limited interest to assess the intrinsic capability of oceanic models in reproducing SSTs. To assess the performance of ocean models in simulating SSTs, they can be run in partially coupled mode (Richter et al. 2012; Wahl et al. 2011). This method consists in correcting one flux send by the atmospheric model to the ocean model, so that the ocean model receives a more realistic flux. The correction can be applied over a limited domain so as to perturb minimally the coupled model. The role of specific atmospheric biases in initiating the SST bias can then be quantified.

Toniazzo (2013) showed the relevance of using initialized coupled experiments to address the mechanisms at the origin of the bias formation in 3 CMIP5 models. The present study is also based on the analysis of initialized experiments but is focussed on the CNRM-CM5 model only. The aim is to quantify the role of the different atmospheric biases in setting the SST biases in the CNRM-CM5 model, and especially to assess their relative importance to drive future improvements of climate models. To estimate the role of atmospheric biases, partially coupled sensitivity experiments in initialized mode have been run using the Wahl et al. (2011) technique. The benefits of analysing the initial drift of sensitivity experiments lie in the analysis of the first order effects and the reduction of the computational cost of these experiments. In Sect. 2, the CNRM-CM5 model is described and its biases in the tropical Atlantic are characterised. The CNRM-CM5 initial drift from a realistic state to its own biased state will be estimated in existing CMIP5 decadal experiments. The next two sections are devoted to the analysis of sensitivity experiments to quantify the relative role of the two main atmospheric biases in the region that contribute to the warm SST bias: the overestimated net surface solar heat flux (Sect. 3) and the atmospheric surface wind (Sect. 4). Section 5 is a discussion of our results, with an assessment of the linearity of atmospheric corrections. Section 6 finally draws the main conclusions of the present study.

2 The CNRM-CM5 model and its biases in the tropical Atlantic

2.1 Model description

CNRM-CM5 was jointly developed by CNRM-GAME (Centre de Recherches Météorologiques-Groupe d'étude de l'Atmosphère Météorologique) and CERFACS (Centre Européen de Recherche et de Formation Avancée) to perform simulations for the CMIP5 exercice. A detailed description of the model is available in Voldoire et al. (2013). The model includes the atmospheric model ARPEGE-Climat (v5.2), the ocean model NEMO (v3.2), the land surface scheme ISBA, the sea-ice model GELATO (v5) and the TRIP river routing model, altogether coupled through the OASIS (V3) software. The horizontal resolution of the atmospheric and land components is 1.4° and the oceanic and sea-ice components are based on an ORCA-1° grid configuration with 42 vertical levels, five levels being in the first 50 m. The atmospheric model is a "low-top" version, with only 31 levels in the troposphere and low stratosphere up to 20 hPa. The models are coupled on a daily time-step. The oceanic surface fluxes are computed following the Exchange Coefficients from Unified Multi-Campaigns Estimates (ECUME, Belamari 2005), which consists in estimating neutral transfer coefficients at 10 m calibrated from five flux campaigns included in the ALBATROS database (Weill et al. 2003).

The origin of the tropical Atlantic SST bias in CNRM-CM5 is addressed using a large set of simulations. Some of them were performed within the CMIP5 framework, such as historical coupled and SST-imposed (or AMIP) experiments and decadal coupled hindcasts. Table 1 summarizes the CNRM-CM5 simulations used in the following.

Table 1 Available CNRM-CM5 simulations used in the present study

Simulation Name	Configuration	Period
AMIP	Atmospheric model forced with HADISST SSTs	1975–2008
HIST	CNRM-CM5 historical simulation	1850–2005
HISTNUD	CNRM-CM5 historical with a nudging of the ocean towards the COMBINE NEMOVAR1 reanalysis	1948–2007
DEC	CNRM-CM5 decadal simulations initialised from HISTNUD	9 start dates 1960,1965,1970,…2000 for 10 years

2.2 Datasets

Various gridded datasets, derived from observations, are used in the present analysis. They are listed in Table 2. Amongst them, the HadISST SST data is the more directly derived from observed data. The surface radiation data (ISCCP_D2 and SRB) is derived from satellite measurements on which a radiation transfer model is applied. Turbulent surface heat fluxes of the HOAPS product are based on satellite measurements while the OAFLUX product makes a more comprehensive use of satellite measurements, ship based observations and reanalysis products. The use of these two datasets give an estimate of the large observational uncertainty associated with surface turbulent heat fluxes. Two reanalysis products are also used: ERA-Interim for the atmosphere and the COMBINE NEMOVAR1 reanalysis for the ocean, both provided by ECMWF. In particular, the COMBINE NEMOVAR1 reanalysis uses the same ocean model, at the same resolution, as CNRM-CM5. The CNRM-CM5 ocean model skills are thus directly comparable to this reanalysis product.

2.3 Tropical Atlantic biases

All CMIP3 models simulate too warm SSTs in the tropical Atlantic basin (Richter and Xie 2008). This bias

Table 2 Datasets derived from observation used in the present study

Product name	Variable used	Method	Reference
HadISST	Sea Surface Temperature	Optimal interpolation	Rayner et al. (2003)
ISCCP_D2	Surface net long-wave and short-wave fluxes	Radiative transfert model using satellite data	Rossow (1996)
SRB			Zhang et al. (2013)
OAFLUX	Surface turbulent heat fluxes	Objective analysis of ship based observations, satellite retrievals and reanalysis	Yu (2008)
HOAPS		Based on SSM/I Satellite retrievals	Fennig (2006)
ERA-Interim (ERA-I)	Surface wind	Reanalysis	Dee et al. (2011)
COMBINE NEMOVAR1	Currents	Reanalysis	Balmaseda et al. (2010)

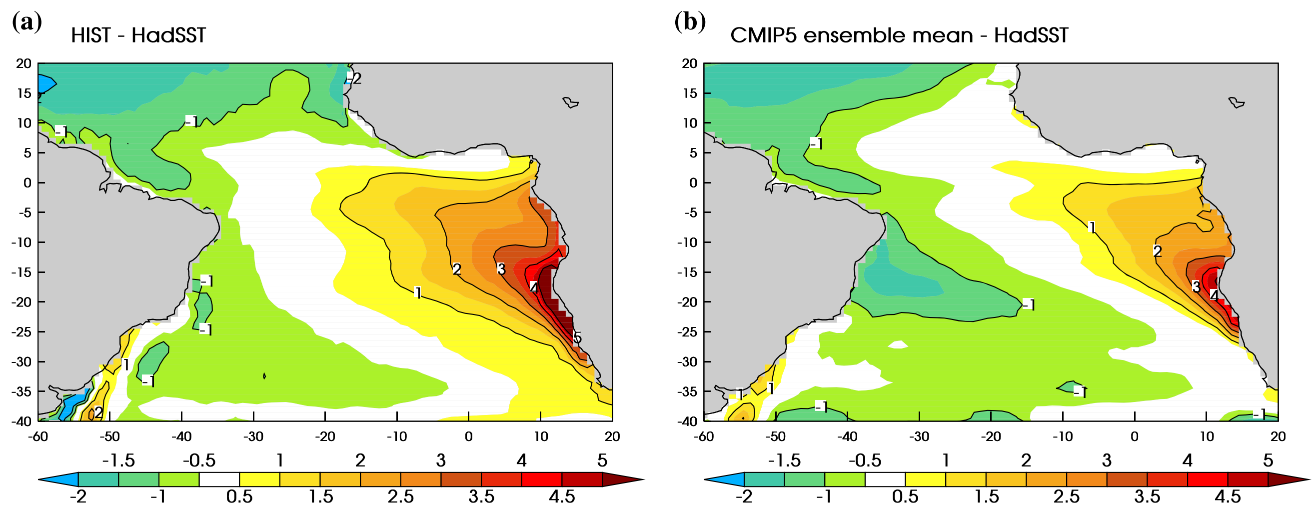

Fig. 1 Difference in annual mean SST (°C) averaged over the period 1970–1999 between historical runs and the HadISST observed data set, **a** for CNRM-CM5, **b** for the ensemble mean of 26 CMIP5 models (ACCESS1-0, CCSM4, CESM1-CAM5, CESM1-FASTCHEM, CMCC-CM, CNRM-CM5, CSIRO-Mk3-6-0, CanCM4, CanESM2, GFDL-CM3, GFDL-ESM2G, GFDL-ESM2M, GISS-E2-H, GISS-E2-R, HadCM3, HadGEM2-CC, HadGEM2-ES, IPSL-CM5A-LR, IPSL-CM5A-MR, IPSL-CM5B-LR, MIROC5, MPI-ESM- LR, MPI-ESM-P, MRI-CGCM3, NorESM1-M, NorESM1-ME)

unfortunately remains robust in the CMIP5 model ensemble (Richter 2013; Roehrig 2013), especially in the CNRM-CM5 model (Fig. 1). On an annual mean basis, CNRM-CM5 simulates a warm bias that extends from the Equator to the southeastern Atlantic. It is most intensive along the African coast: from 0 to 40°S along the coast, the warm bias exceeds 3 °C and reaches 5 °C near 20°S. The pattern of the bias is very similar in the CMIP5 ensemble mean, though slightly small in the latter's, suggesting that some models perform better than CNRM-CM5 over the region.

In the tropical Atlantic, the warm bias is generally attributed to the misrepresentation of the amplitude of the SST annual cycle, directly associated with the intense spring cooling of the Atlantic Cold Tongue (ACT). This spring cooling can be diagnosed with the difference between July and April mean SST, as shown in Fig. 2a for the HadISST dataset. The cooling exceeds 5 °C between 20°S and the Equator along the African coast and extends westward along the equator as far as 20°W. In the CNRM-CM5 model (Fig. 2b), the net cooling in the eastern equatorial region is very weak, and becomes stronger westwards, contrary to observations. The most intense cooling reaches 5 °C offshore the Angola coast south of 20°S. In the CMIP5 multi-model mean (Fig. 2c), the ACT pattern is not reproduced. The cooling along the Equator is weak and more intense in the central/western basin than in the eastern part. It should be acknowledged that the ensemble mean of several models could hardly reproduce the observed sharp gradients. The bias is displayed in Fig. 2c and d and pictures a warm anomaly in the eastern equatorial Atlantic and in the Gulf of Guinea. This pattern differs from the annual mean bias (Fig. 1), which is not very intense in the Gulf of Guinea but maximum near 20°S along the coast. CNRM-CM5, as well as most of CMIP5 models, thus does not capture properly the ACT. On the contrary, the seasonal cooling at 20°S along the African continent, attributed to coastal upwelling, is better simulated in the CNRM-CM5 model. To analyse the SST biases in the tropical Atlantic, two regions need to be distinguished, and both the amplitude of the annual cycle and the annual mean bias have to be considered, as they do not appear equivalent. The relationship between these two facets will be partly addressed in the following.

2.4 Initial drift in decadal experiments

The tropical Atlantic SST bias is analysed in the following using coupled simulations, initialized as close as possible from observations. As in Toniazzo (2013), we took advantage of the decadal hindcasts performed within the CMIP5 exercise. In the CMIP5 context, there was no recommendation on the way to initialise models for decadal hindcasts. Generally, only the ocean component of the system is initialised since it is supposed to be the primary source of predictability in the climate system at the decadal scale.

In the present study, the CNRM-CM5 ocean component is initialised using the COMBINE NEMOVAR1 reanalysis, performed with the same configuration of NEMO. However, the direct initialisation of the ocean state by the reanalysis generates instabilities in the coupled system. An intermediate coupled simulation is thus performed, in

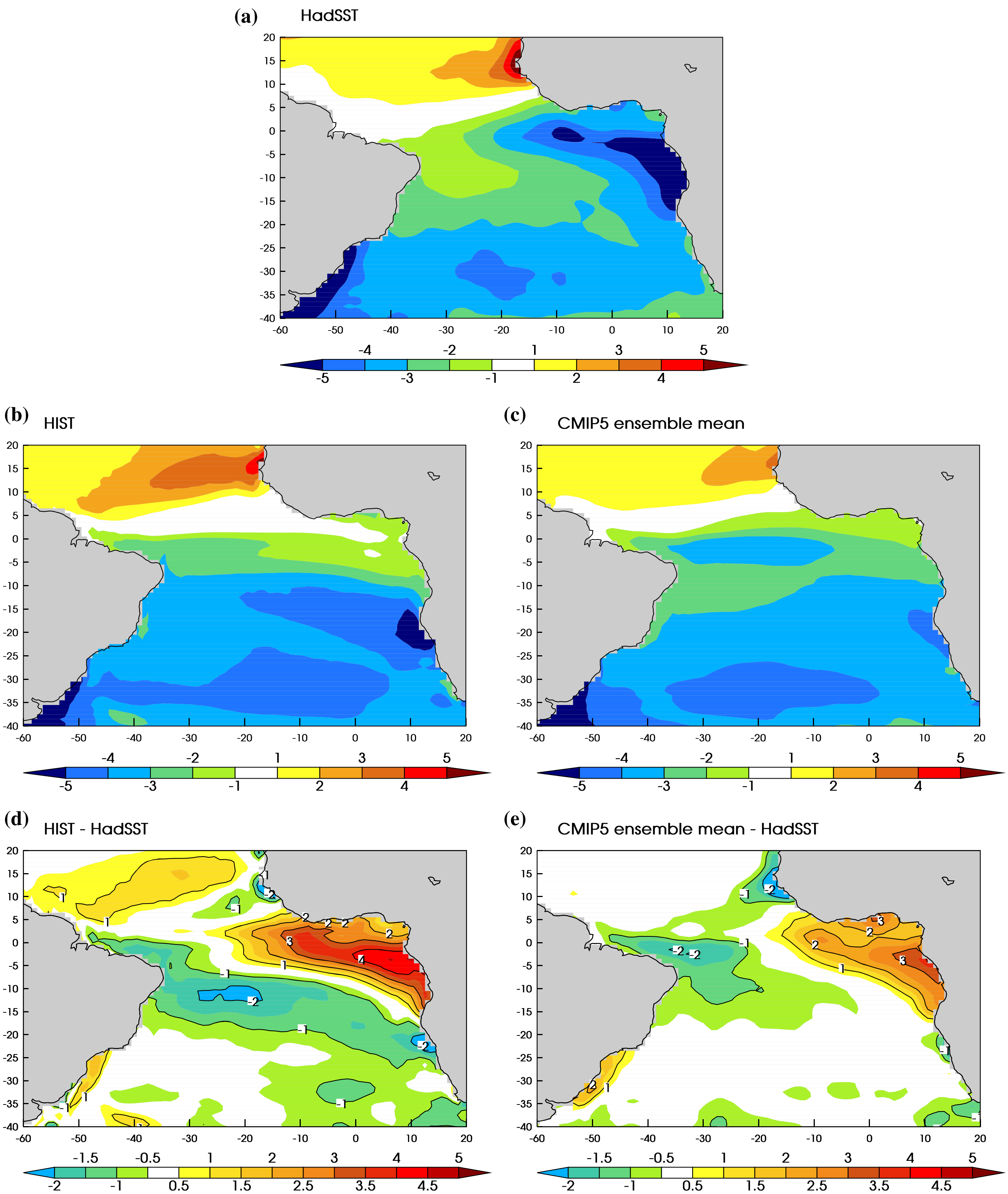

Fig. 2 July minus April mean SST difference (°C) averaged over 1970–1999 for **a** the HadISST observed data, **b** the CNRM-CM5 model and **c** the ensemble mean of 26 CMIP5 models. Difference in spring cooling between d) the CNRM-CM5 model and the HadISST data and (i.e. **b**, **a**) **e** between the CMIP5 ensemble mean and the HadISST data (i.e. **c**, **a**)

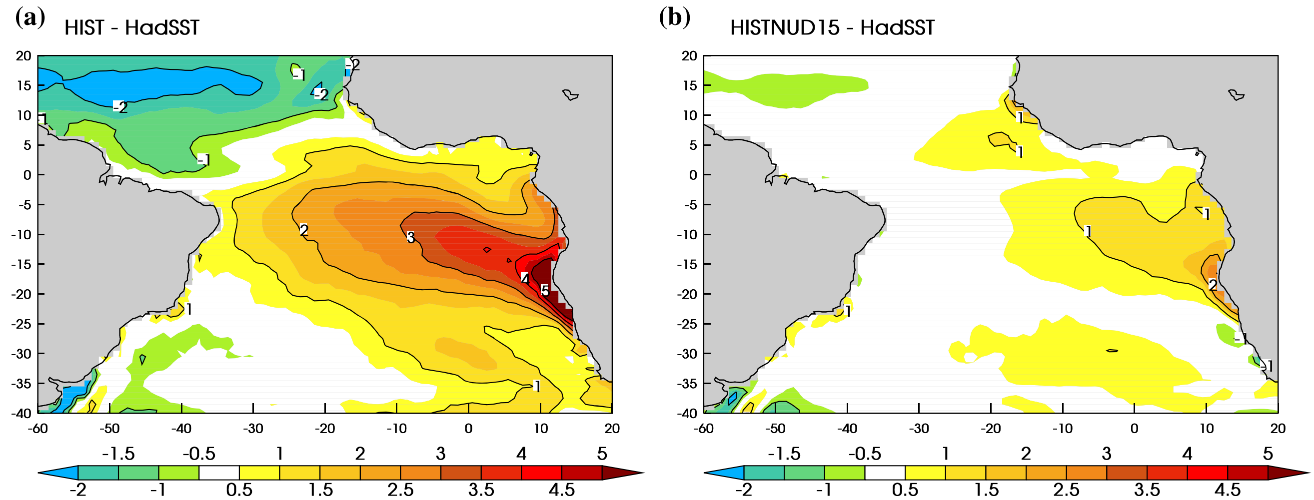

Fig. 3 January mean bias in SST (°C) in the historical simulation and in the HISTNUD simulation averaged over the period 1970–1999 using HadISST as reference

which surface temperature and salinity are restored to the NEMOVAR1 reanalysis, using the Barnier et al. (1995) flux correction with a relaxation coefficient of 40 W m^{-2} K^{-1}. In this simulation, the deep-ocean is also nudged towards the NEMOVAR1 reanalysis monthly data outside the 15°S–15°N region, with a 10 days relaxation frequency between the mixed layer and 800 m and with a 1 year relaxation frequency below. This nudged simulation (called HISTNUD, see Table 1) provides initial conditions for the decadal hindcasts, on January the 1st every 5 years between 1960 and 2005. The decadal simulations are run for 10 years without any restoring. An ensemble of ten members, differing only by their initial atmospheric states, was built to quantify the model internal variability. It was checked that the initial states provided by HISTNUD are much more realistic compared to observations than the equilibrium state of the coupled model HIST (Fig. 3), although a weak warm bias remains in the southeastern part of the basin. The SST restoring is probably not sufficient to fully correct biases of the ocean model itself.

After 2 months, in March, the bias of the decadal hindcast (DEC hereafter) is much larger than the bias in HISTNUD (Fig. 4). The Atlantic SST bias thus develops quickly. The time-scale of the drift is assessed on Fig. 5, using on the one hand the distance (root mean square error of the SST) between DEC and HISTNUD, and on the other the distance between DEC and HIST. DEC is expected to get closer (farther) to HIST (HISTNUD) as time increases. The distance is normalized by the distance between HISTNUD and HIST to remove the bias annual cycle. Huang et al. (2007) show that the bias has a seasonal cycle and peaks in autumn. However, only simulations initialised in January are used and thus do not account for the respective roles of the bias seasonality and the lead-time effect. In January, the DEC simulations are closer to HISTNUD than HIST, as a result of the initialization. In February, the DEC simulations already becomes closer to HIST than HISTNUD, indicating that the tropical Atlantic SST warm bias has already settled down after less than 2 months. This fast initial drift is robust whatever domain, variable, year of initialisation and ensemble member is chosen (not shown). Toniazzo (2013) assess the initial evolution of SSTs in 3 CMIP5 models and find a similar quasi immediate strong warming only in the CFSv2 model.

The decadal hindcast protocol is thus relevant to further analyse the tropical Atlantic SST biases. It will be used in the following to investigate the respective role of atmospheric biases in the development of the CNRM-CM5 biases in the tropical Atlantic.

2.5 Role of atmospheric fluxes

Within the CNRM-CM5 coupled model, the atmospheric component sends to the ocean component three surface fluxes: the net solar heat flux, the non-solar heat flux and the wind stress. The net non-solar heat flux is the sum of the net long-wave radiation, the latent heat flux and the sensible heat flux, but the ocean model does not make use of this partition. Biases in the net solar heat flux and wind stress over the tropical Atlantic have been emphasized in several studies as possible explanations of the warm SST bias in coupled model (e.g., Richter and Xie 2008; Wahl et al. 2011). Before testing their role in the CNRM-CM5 model, using the idealized framework of decadal hindcasts, the flux biases are first quantified hereafter, following the partition used by the ocean model.

The net surface solar heat flux simulated by the CNRM-CM5 model is negatively biased in the equatorial region

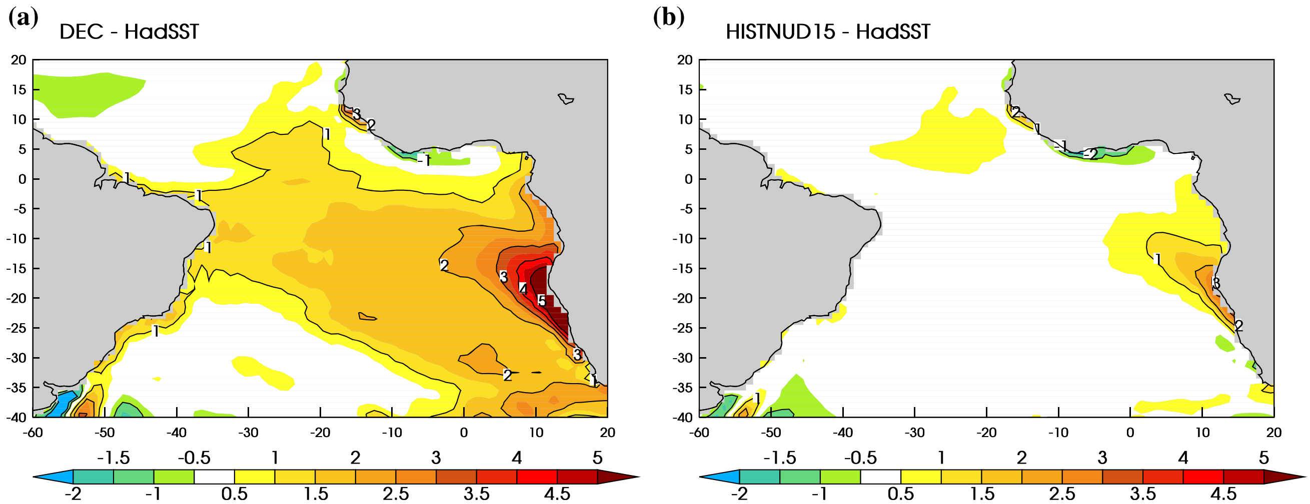

Fig. 4 March mean bias in SST (°C) in the first year of the decadal simulation and in the HISTNUD simulation averaged over the period 1970–1999 using HadISST as reference

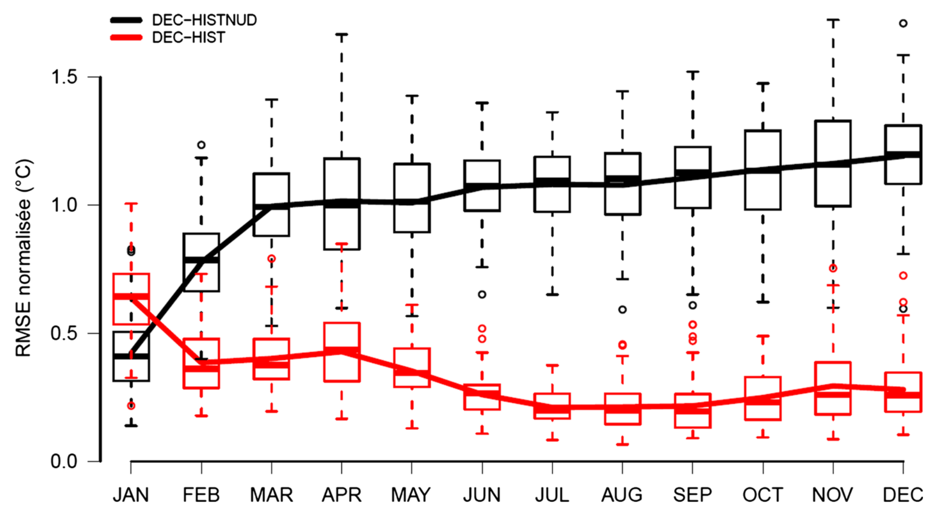

Fig. 5 Distance RMSE(DECADAL-REF)/RMSE(HISTNUD-historical) with REF = HISTNUD in black and REF = historical in red over the domain 20S-2S, 0E − 15E for SST. The distance is calculated for each simulation member of the decadal simulation and for each start year. The box and whisker indicates the mean distance averaged over all members, the 1st and 3rd quartiles as well as the min and max of the ensemble distribution

(Fig. 6a), being a cooling source for the ocean. Along the Equator, this bias remains negative all year long (not shown). On the opposite, the net solar heat flux is overestimated in the southeastern tropical Atlantic, especially from June to January, when it exceeds 50 W m^{-2} on average over this region (Fig. 6c). Despite the large uncertainty in the retrievals of the net surface solar heat fluxes, the positive bias of CNRM-CM5 remains robust and of several tenths of W m^{-2}, whatever radiation product is used for comparison (Fig. 6c). The pattern and amplitude of this bias is very similar to that obtained from an AMIP experiment with CNRM-CM5, where SSTs are prescribed to the HadISST observed values. Only the pattern along the Equator is changed, indicating feedbacks in the model between the atmosphere and the ocean there. The location and amplitude of the positive bias is remarkably similar between the DEC and AMIP simulations, implying that the bias is rather intrinsic to the atmospheric model than related to coupling feedbacks between the two model components. The CNRM-CM5 has been shown to be strongly lacking of stratocumulus and stratus clouds in the eastern part of tropical ocean basins (Césana and Chepfer 2012). As a consequence, the shortwave cloud radiative effect is strongly underestimated (Voldoire et al. 2013), so that the CNRM-CM5 positive bias in the net surface solar heat flux in the southeastern tropical Atlantic is, to a large extent, due to the cloud component of the radiation budget. Note also that the CCSM4 model, analysed in Grodsky et al. (2012), shares high similarities with CNRM-CM5 regarding the location, intensity and seasonality of the net surface solar flux bias. Even if few models are now able to represent stratocumulus in the tropics, Klein et al. (2013) and Su et al. (2013) have shown that this flaw is still present in most of CMIP5 models.

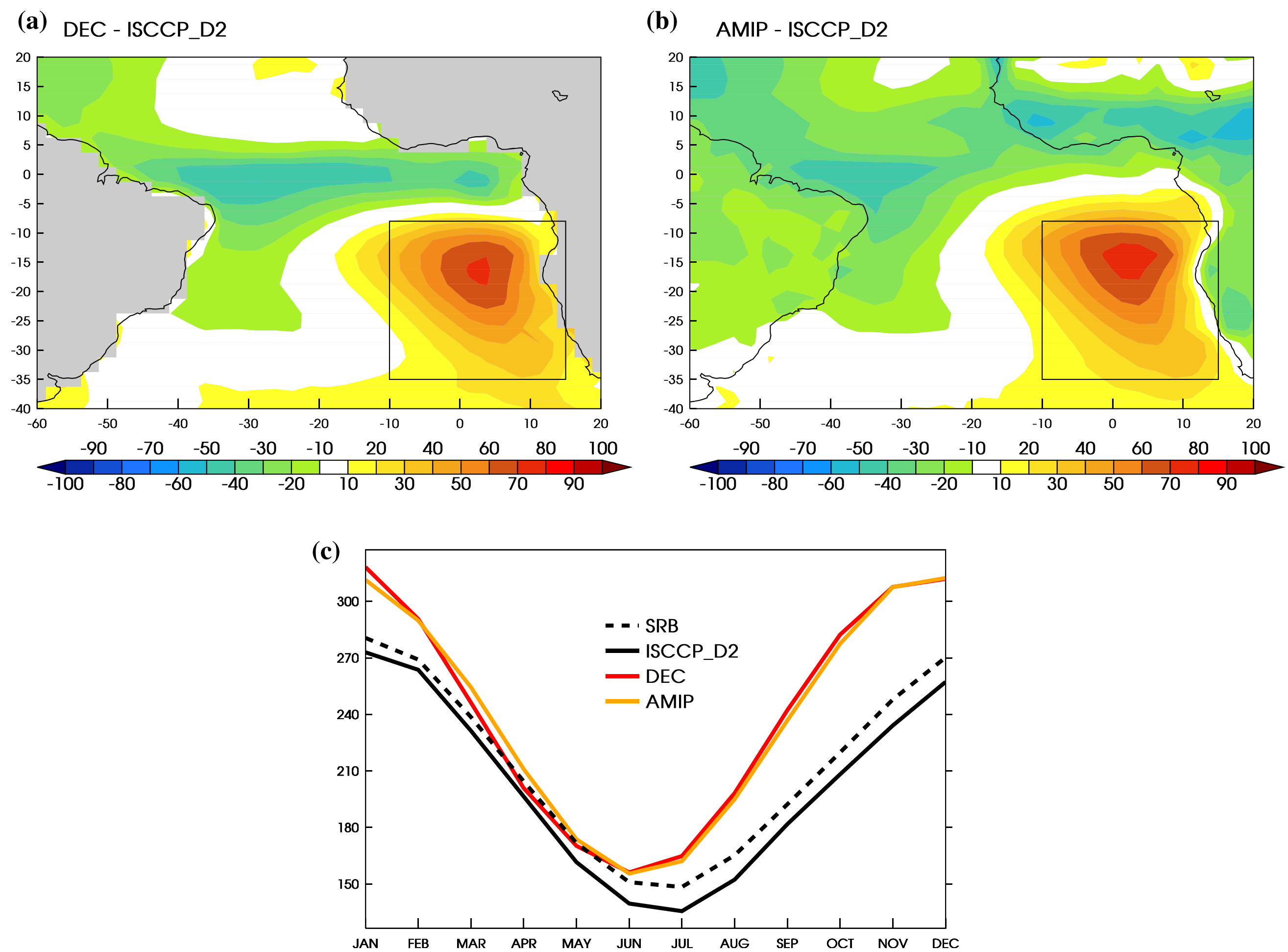

Fig. 6 Annual mean bias in net solar heat flux (W m^{-2}) at the ocean surface for **a** the first year of decadal simulations (all start date and members considered), **b** an AMIP type experiment done with the same version of the atmospheric model, **c** annual mean cycle of the net solar heat flux averaged over the region 10W–15E, 35S–8S (indicated as a *box* on figures **a** and **b**) for several reference observed data set (isccp_d2 and SRB), for the first year of decadal experiments and for the AMIP experiment

The net non-solar surface heat flux is mainly negatively biased all over the domain (Fig. 7a), inducing a cooling of SSTs, strongest in the southeastern tropical Atlantic. There, it acts as a negative feedback, partly compensating the positive bias in the shortwave. Note that the amplitudes of the positive solar and negative non-solar biases cannot be quantitatively compared, as the datasets used here do not allow a proper closure of the surface energy budget. However, whatever combination of radiation and turbulent flux retrievals is used, the CNRM-CM5 bias remains negative all year long, beyond the uncertainties associated to observational products (Fig. 7c). The negative bias is reduced in the AMIP experiment by 20–30 W m^{-2} on average, as observed SSTs partly improve the longwave radiation at surface as well as the latent heat flux. It however remains negative compared to observations, indicating that the non-solar heat flux is likely not a direct cause of the warm SST bias initiation. Therefore, the role of the net non-solar heat flux will not be further investigated in the following, even though it clearly feedbacks with the SST bias.

Wind stress is directly derived from surface wind, whose observations are assimilated in the ERA-Interim reanalysis. Therefore, ERA-Interim surface winds can be used as a reference to quantify surface winds biases. Over the tropical Atlantic, climate model wind biases in spring have been shown to be an important source of SST biases (Chang et al. 2007; Richter and Xie 2008). We will thus focus on the March–April–May season. If the large-scale wind structure seems rather well captured, CNRM-CM5 underestimates the zonal wind in the equatorial Atlantic, especially from 10°S to the Equator (Fig. 8a). The wind intensity underestimate is the largest west of 10°W where it reaches 5 m s^{-1}. Such a zonal wind bias has significant consequences on the ocean upper-layer temperatures because the zonal wind stress induces upwelling (Caniaux

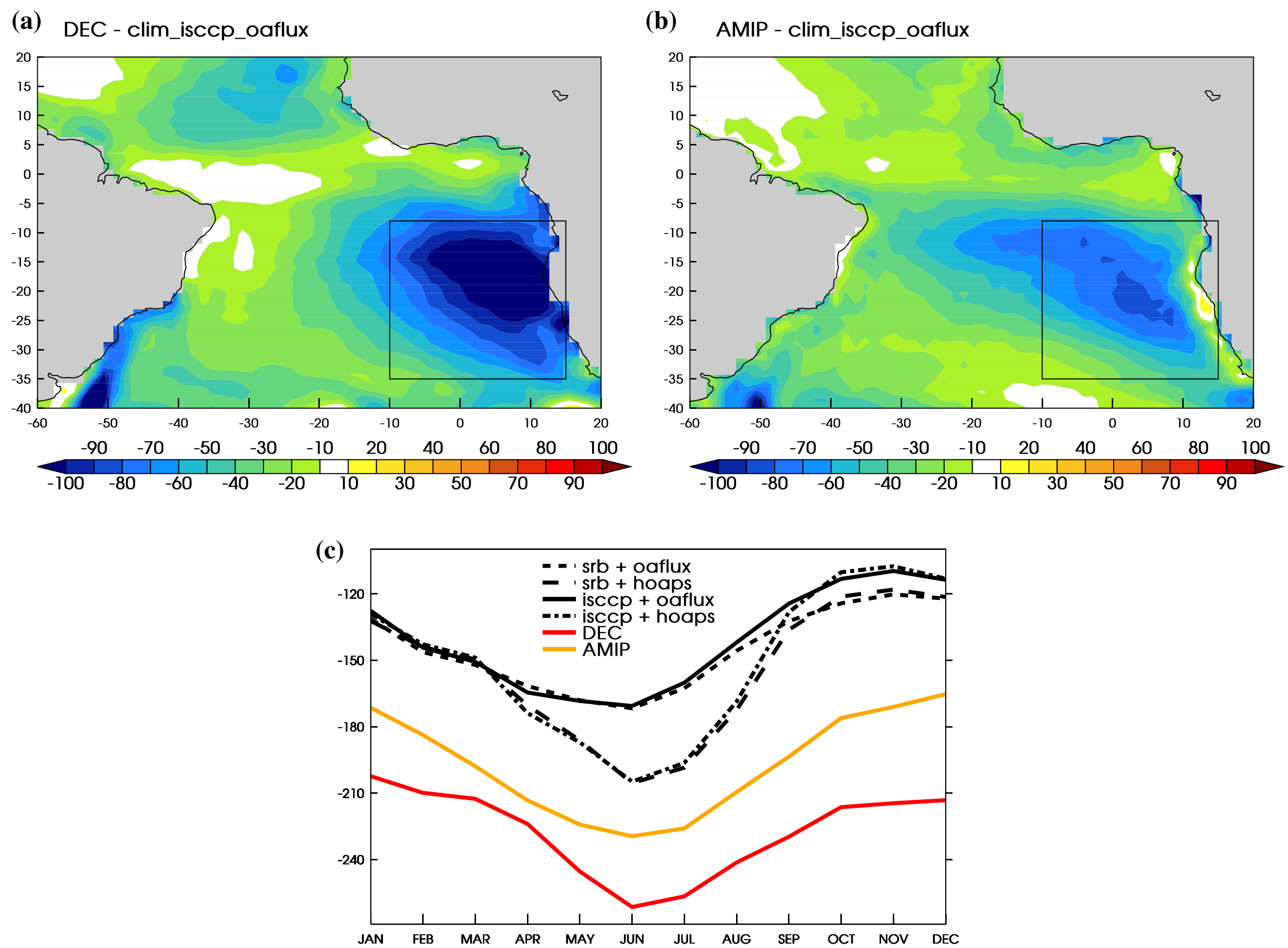

Fig. 7 Same as Fig. 5 for the non solar heat flux. For **a** and **b** the reference data is oaflux for sensible and latent heat flux and isccp-d2 for the net long-wave flux. For **c**, all combinations between oaflux/hoaps for turbulent fluxes and isccp-d2/SRB for long-wave flux are indicated

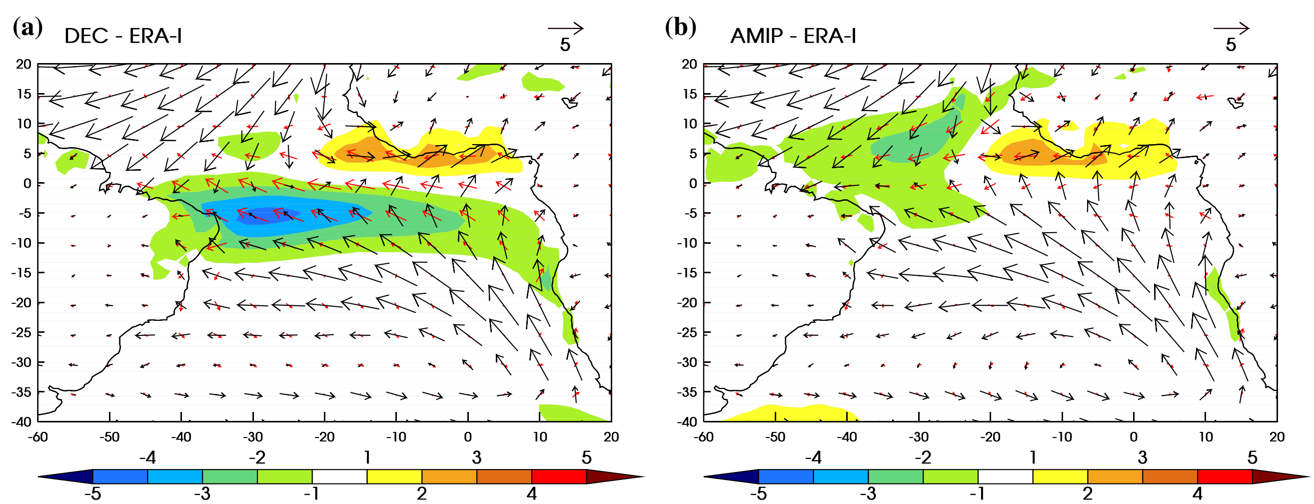

Fig. 8 Surface wind (m s^{-1}) in March–April–May for **a** the first year of decadal simulations (all start date and members considered), **b** an AMIP type experiment done with the same version of the atmospheric model. *Black vectors* indicate the simulated wind, and the red vectors are the difference between the ERA-Interim reference and the simulated wind (they consequently indicate the direction and intensity that should be added to the simulated wind to obtain the reference). *Shading* indicate the wind intensity bias between the simulations and the ERA-Interim reference

Table 3 Sensitivity experiments and their characteristics

<table>
<tr><th>Experiment Name</th><th>Region of solar correction</th><th>Region of Wind correction</th><th>Components of the wind corrected</th><th>Data used as reference</th></tr>
<tr><td>SSC</td><td>10W-15E, 8S-35S</td><td></td><td></td><td>ISCCP-D2</td></tr>
<tr><td>EQ-UV</td><td></td><td rowspan="2">40W-10E, 1.5S-1.5N</td><td>U and V</td><td rowspan="4">ERA-Interim</td></tr>
<tr><td>EQ-U</td><td></td><td>U</td></tr>
<tr><td>COAST-UV</td><td></td><td>2W-15E, 20S-1.5N</td><td>U and V</td></tr>
<tr><td>ADD</td><td>10W-15E, 8S-35S</td><td>40W-10E, 1.5S-1.5N</td><td>U and V</td></tr>
<tr><td>EQ-UV-AMIP</td><td></td><td>40W-10E, 1.5S-1.5N</td><td>U and V</td><td>AMIP</td></tr>
</table>

et al. 2011; Giordani and Caniaux 2011) and turbulent mixing (Foltz et al. 2003; Wade et al. 2011; Giordani et al. 2013), which are the major sources of cooling for the ACT. In the forced experiment (Fig. 8b), the biases are reduced south of the Equator and the southeasterly trade winds are better represented, in particular regarding their intensity. Only remains the underestimate of the northern trade winds intensity between 5°N and 15°N.

To better quantify the respective role to the two main atmospheric biases that contributes to the warm SST bias in the tropical Atlantic, in terms of both mean state and annual cycle, sensitivity experiments (Table 3) have been performed using the decadal hindcast protocol and idealized corrections of the net surface solar heat flux and wind stress. They are analysed in the next two sections.

3 Role of the surface solar heat flux

3.1 Design of the sensitivity experiment

The location of the net solar heat flux excess is stable over the years and seasons. A negative corrective term is uniformly added over the fixed limited oceanic region [10°W–15°E, 35°S–8°S] (Fig. 6), in order to reduce the shortwave energy received by the ocean model. The correction is estimated as the averaged bias of DEC compared to the ISCCP-D2 data over this region on a monthly basis. It is then interpolated on a daily time-step to avoid abrupt changes in the correction and directly applied to the ocean model. This sensitivity experiment, following the DEC protocol, is called SSC (Table 3). The initial drift in DEC in the tropical Atlantic develops in a very similar way for each member or start year. To limit computational cost, an ensemble of only three 1-year members is run for the start year 1995. Significance of the sensitivity experiment results in comparison to those of the DEC experiment will be evaluated using a two-tailed Student's t test.

3.2 Results

The effect of the surface shortwave radiative flux correction in the SSC experiment is to reduce the mean SSTs from 1 to 2 °C over the domain where the correction is applied (Fig. 9a). The effect is maximum and significant at the 95 % level over all the south tropical Atlantic. The SST cooling is significant west and north of the corrected region, suggesting that the cooler waters are advected there. Figure 9b indicates that the net solar heat flux correction yields a significant increase of the spring cooling over the eastern equatorial Atlantic, north of the corrected domain. Thus the weak spring cooling in the coupled model (DEC or HIST) partially results from non-local biases. The annual cycle of SSTs in the southeastern tropical Atlantic is also improved (Fig. 10). SSTs are reduced all year long, especially after the Spring cooling when the bias reduction reaches 1.5 °C. Note that SSTs are reduced in January during the first month of simulation, emphasizing that the impact of the net solar heat flux correction is very fast. Moreover, all three members are cooler than their counterpart in DEC, underlining the robustness of the response.

4 Role of the surface wind

4.1 Design of the sensitivity experiments

The surface wind will be corrected using a regional nudging technique. While it directly impacts the atmospheric model in contrary to the SSC experiment, its advantage lies in that surface turbulent fluxes are calculated using a more realistic wind, keeping the different surface

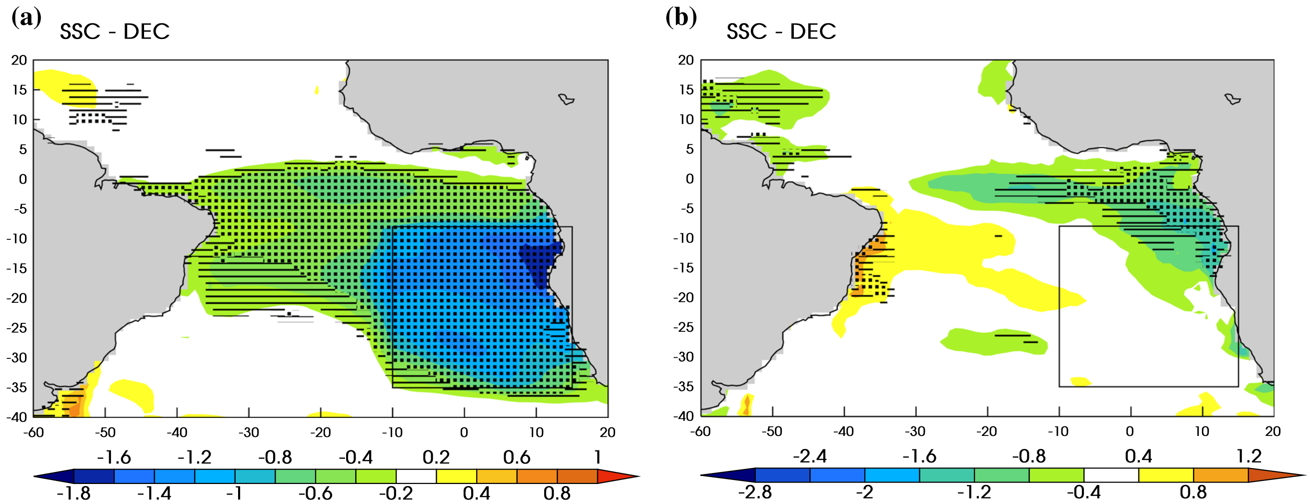

Fig. 9 **a** Difference in annual mean SST (°C) between experiment SSC and the reference decadal experiment. **b** Difference in spring SST cooling between SSC and the decadal experiment calculated as in Fig. 2 as the difference between July and April SSTs. Simulations are ensemble of three members starting in January 1995 (only these members of the decadal simulations are considered here). The *box* indicate the region of solar heat flux correction. Black shading indicates the regions of significant SST change at the confidence level 95 % (*horizontal lines*) and 99 % (criss-cross layout) according to a two-tailed Student t test

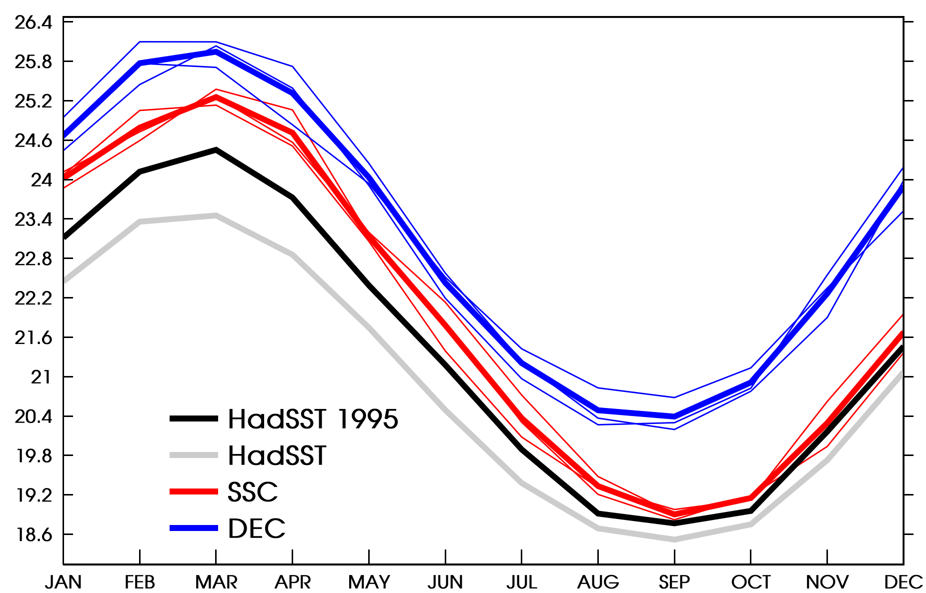

Fig. 10 Annual cycle of SSTs (°C) over **a** the box 35S–8S, 10W–15E used in experiment SSC for the HadISST data for year 1995, the HadISST data averaged over the period 1970–1999, the SSC and decadal experiment (DEC) averaged over the ensemble of three members started in January 1995 (*thick line*) and each member (*thin line*)

heat fluxes consistent. Spurious effects in transition zones from nudged to free regions are limited by prescribing a vertical profile of the relaxation time which decreases from 1 h at the first atmospheric model level to zero at the 6th level (around 850 hPa). In the horizontal directions, a sponge zone of three grid points (4.5°) is used to reduce to zero the relaxation time. As for the SSC experiment, an ensemble of only 3 1-year members is run from the starting year 1995.

Several sensitivity experiments have been performed. They are listed in Table 3. In Richter et al. (2012) and Wahl et al. (2011), the equatorial winds have been shown to be of primary importance to reduce the SST bias. The first sensitivity experiment, called EQ-UV, nudges the surface wind along the Equator between 1.5°S and 1.5°N. A complementary experiment where only the zonal wind is nudged (EQ-U) is performed to analyse the role of wind components. Grodsky et al. (2012) show that the wind in the southeastern tropical Atlantic is also crucial. A third sensitivity experiment (EQ-COAST) is thus performed by nudging the wind over the region [2°N–20°S, 0°E–15°E]. In all these experiments, the wind is nudged towards the ERA-Interim climatological wind, defined as the mean annual cycle over the period 1989–2008, smoothed using a

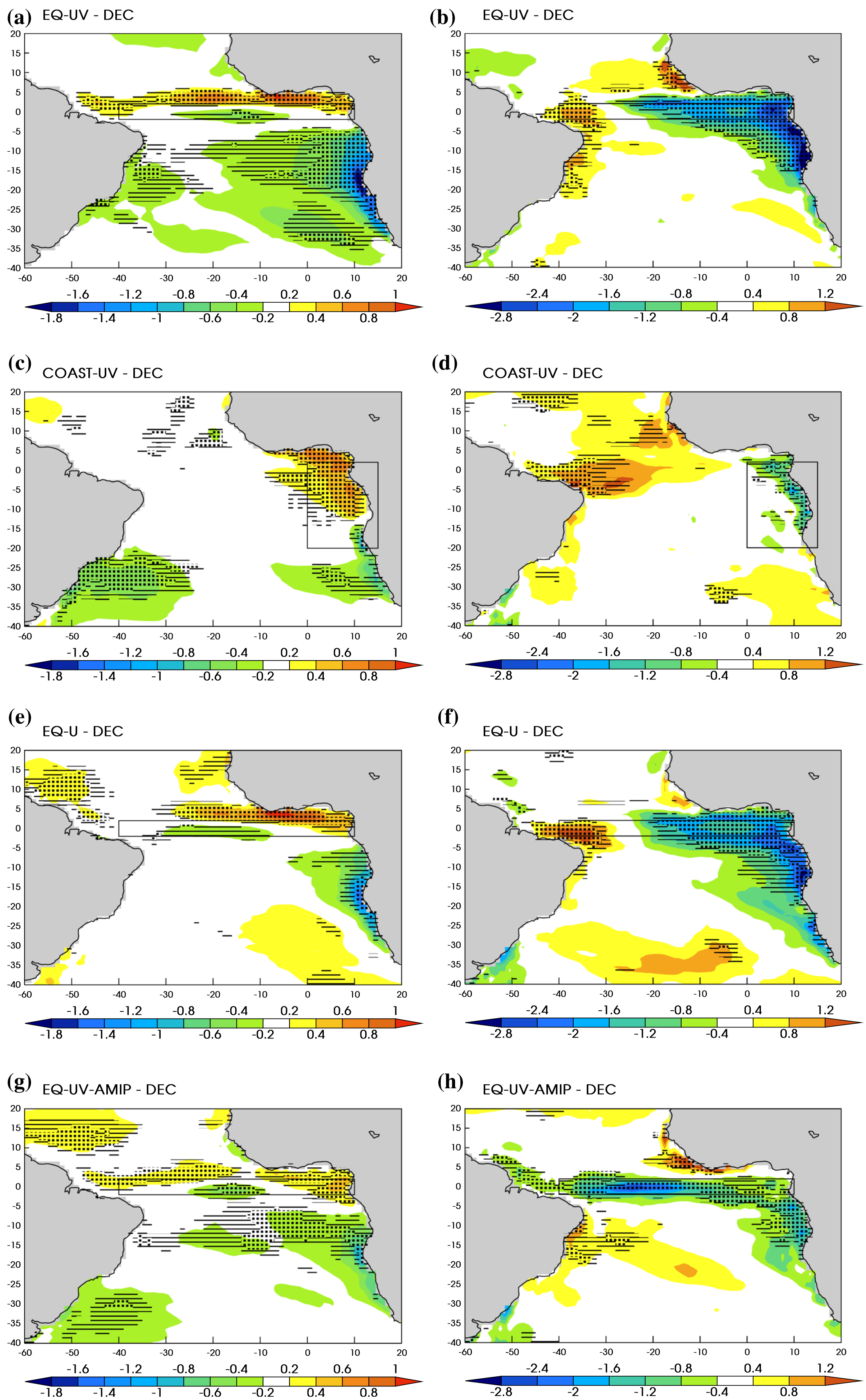

Fig. 11 Same as Fig. 9 for **a**, **b** experiment EQ-UV, **c**, **d** COAST-UV, **e**, **f** EQ-U, **g**, **h** EQ-UV-AMIP

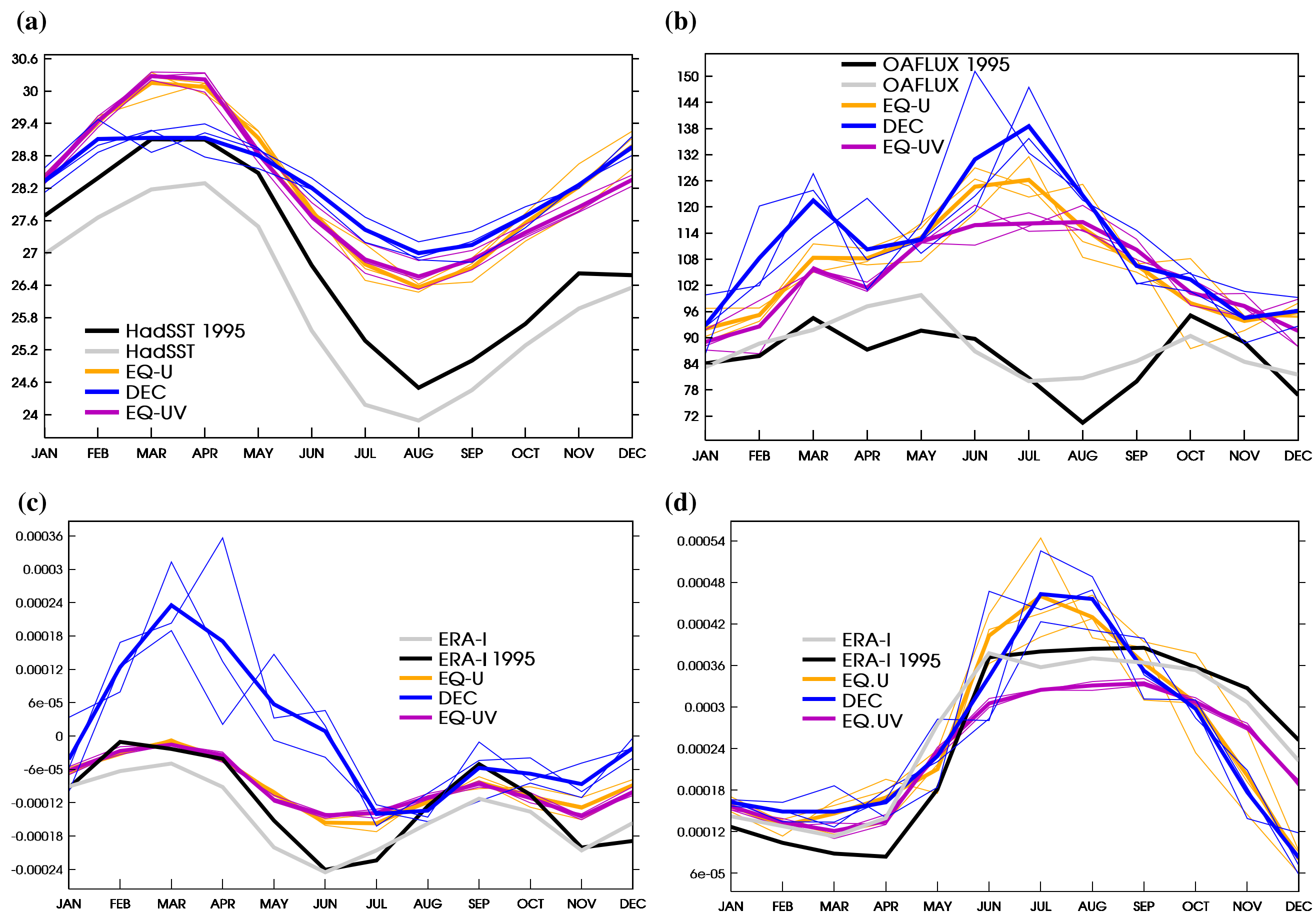

Fig. 12 **a** Annual cycle of SSTs (°C) averaged over the ATL3 box 3S–3N, 20W–0E for the HadISST data for year 1995, the HadISST data averaged over the period 1970–1999, the reference decadal experiment (DEC in *blue*), the EQ-UV experiment (*orange*) and the EQ-U experiment (*purple*). Same for **b** latent heat flux (W m^{-2}) with reference OAFLUX, **c** zonal surface wind stress (N m^{-2}) and **d** meridional surface wind stress (N m^{-2}) both with reference ERA-Interim. Ensemble members are indicated by *thin lines* and ensemble mean by *thick lines*. *Black lines* indicate annual mean cycle of reference datasets

31-day running average. Finally, the role of the coupling is analysed through another experiment (EQ-UV-AMIP), similar to EQ-UV, but where the reference wind comes from the AMIP CNRM-CM5 simulation averaged over the period 1979–2008.

4.2 Results

The nudging of the surface wind in the Atlantic equatorial band (EQ-UV) has a weak but significant impact on the mean SST in the equatorial region where the nudging is applied (Fig. 11a). SST biases are only reduced in autumn; not in summer and even amplified in spring (Fig. 12a), so that the mean bias remains quasi unchanged. On the opposite, the equatorial wind correction strongly intensifies the spring cooling by more than 2 °C along the Equator and south of it along the African coast (Fig. 11b). This suggests that the wind stress has an impact on the spring cooling mechanism but not on the mean state. In spring, correcting surface winds also corrects zonal surface wind stress sign and intensity (Fig. 12c), which may explain the reduction of latent heat flux (Fig. 12b). As other surface heat fluxes are not affected, the overestimated latent heat flux along the year likely explains the SST positive bias.

The wind correction in the coastal domain in COAST-UV induces a weak warming of annual mean SSTs in the Gulf of Guinea (Fig. 11c). The effect on the spring cooling is weak but significant along the coast (Fig. 11d). Equatorial winds are thus crucial for the simulation of a realistic spring cooling. Corrected equatorial winds (EQ-UV) also tend to reduce the warm bias along the southeastern African coast, which is consistent with Richter et al. (2012). They attributed this remote effect to changes in the oceanic circulation via equatorial and coastal Kelvin waves. The wind correction also improves in their model the representation of the subtropical anticyclone and along-shore winds, which has a

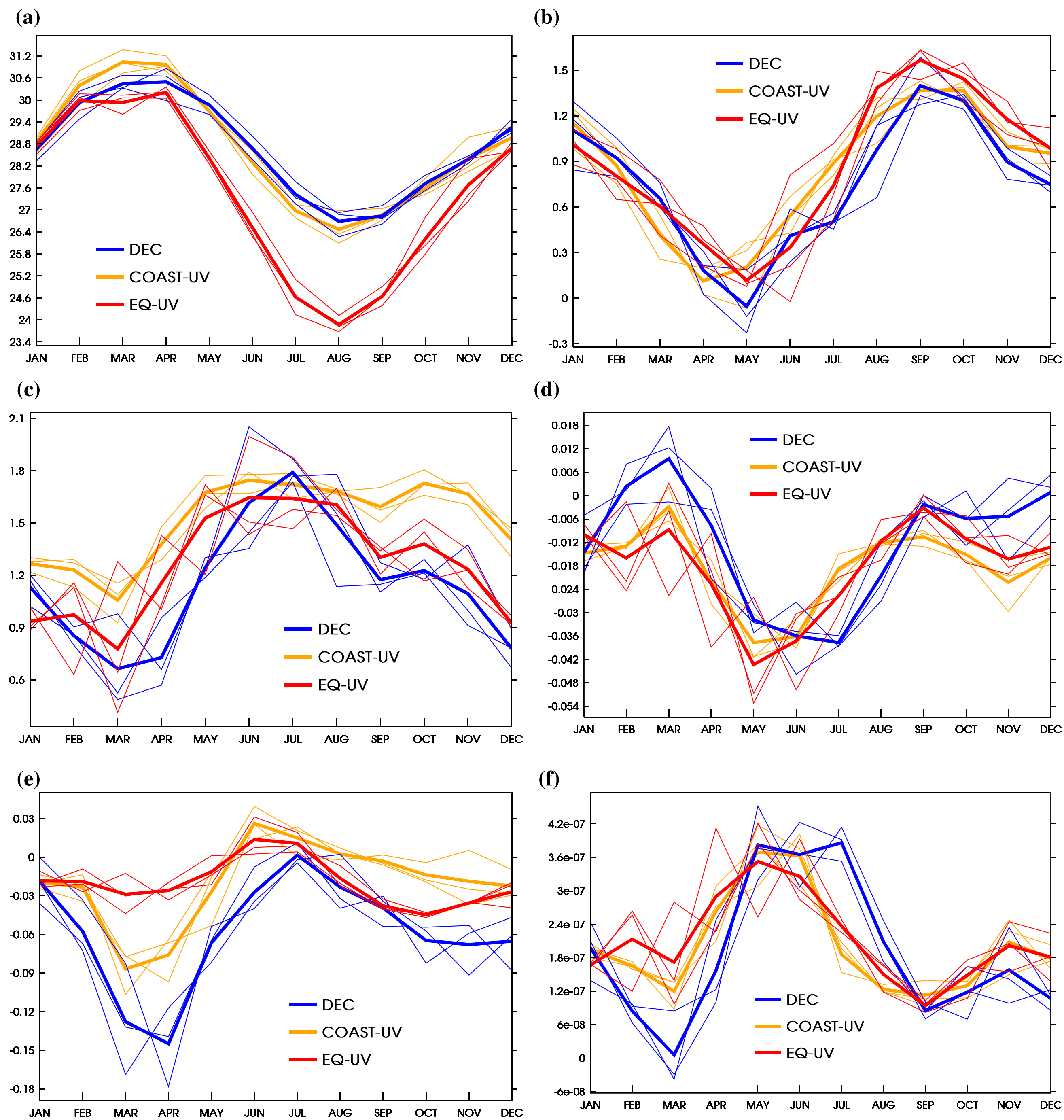

Fig. 13 Annual cycle of **a** SSTs (°C), **b** zonal surface wind (m s^{-1}), **c** meridional surface wind (m s^{-1}), **d** zonal surface current (m s^{-1}) **e** meridional surface current (m s^{-1}) and **f** surface current divergence (s^{-1}) averaged over the box 20S–2S, 10E–15E for the reference decadal experiment (DEC in *blue*), the EQUV experiment (*red*) and the COAST-UV experiment (*orange*). Ensemble members are indicated by *thin lines* and ensemble mean by *thick lines*

direct impact on the oceanic circulation. Surprisingly, and in contrary to the results of Richter et al. (2012), the wind bias in the southeastern tropical Atlantic only reduce SST by 1° south of 15°S along the coast in a region where the warm bias exceeds 5 °C. This indicates that the primary source of error in this region might depend on the model.

As in Wahl et al. (2011), the annual mean SST bias reduction in EQ-UV in the coastal region likely implies remote effects from the nudging domain (Fig. 11a). In their study, the cooling in the southeast tropical Atlantic positively feedbacks via an increase of cloud cover. On the opposite, the SST cooling in CNRM-CM5 does not have any significant impact on cloud cover, suggesting an unrealistic SST-cloud feedback in the model.

To explain this remote effect, two hypotheses, possibly combined, can be proposed: (1) the equatorial nudging has modified the large-scale atmospheric circulation over the tropical Atlantic, so that currents and upwelling in the Southeast have intensified due to atmospheric changes; (2) the equatorial ocean circulation has been locally modified, leading to a non-local ocean circulation response close to the coast. In fact, only the meridian surface current in the southeastern tropical Atlantic is modified between the DEC and EQ-UV simulations (Fig. 13). Atmospheric surface winds and the zonal surface current in this region remain pretty similar between the two experiments. The remote impact on coastal SSTs in EQ-UV is a consequence of modifications in the large-scale ocean circulation rather than in the large-scale atmosphere circulation.

Figure 14 emphasizes these changes in the equatorial zonal ocean circulation, zoomed in the layers between the surface and the 180-m depth. In the NEMOVAR1 reanalysis (Fig. 14b), the westward South Equatorial Current (SEC) extends between the surface and 20-30 m. Underneath, the eastward Equatorial Undercurrent (EUC) is located at a 60-m depth, and covers most of the basin in longitude. Accordingly, the mixed layer is shallow along the Equator, and slightly deeper in the western part of the basin, as shown in de Boyer-Montégut et al. (2004). A comparison with the PIRATA buoy data (Bourlès et al., 2008) located at 0°N–23°W indicates that the EUC depth is correctly captured in the NEMOVAR1 reanalysis, despite an underestimate of its amplitude by 40 %. Although the DEC experiment is using the same ocean model as the NEMOVAR1 reanalysis, it fails in capturing the surface ocean circulation along the Equator (Fig. 14a). No SEC is simulated and the EUC extends from the surface to 60-m depth. A narrow westward current can be found in the easternmost part of the basin, but it remains confined near the coast. The representation of the oceanic currents in DEC is clearly unrealistic, similarly to the GFDL coupled model used in Richter et al. (2012).

The nudging of the surface wind along the Equator strongly improved the representation of equatorial zonal currents (Fig. 14c). The main features of the ocean circulation are corrected, even if the EUC intensity remains under-estimated. Consequently, the mixed layer depth is better simulated. However, the west-east gradient is over-estimated compared with De Boyer-Montégut et al. (2004). The thermocline structure is rather similar to that of the NEMOVAR1 reanalysis, suggesting that EQ-UV achieves the best that can be with this ocean model at this resolution. The change in surface meridional current along the African coast (Fig. 13e) is probably a consequence of the ocean equatorial circulation improvements. The SEC generates divergence along the coast at the Equator, which favours a northward meridional current anomaly there. Divergence is also increased southward along the African coast (Fig. 13f). According to the Ekman theory, the increased divergence promotes local upwelling.

In the COAST-UV experiment, equatorial zonal surface currents are slightly improved locally, where the wind is corrected, but the correction effect remains limited to the coastal region, with no extension to the west (Fig. 14e). No clear reduction in annual mean SST bias along the coast is observed either (Figs. 11c and 13a). The equatorial zonal currents are thus better simulated in EQ-UV because the wind-stress is locally more realistic. In COAST-UV, the nudging locally impacts on the meridional current, in a slightly weaker way than in EQ-UV, especially in spring (Fig. 13d–e). The local wind forcing has thus a smaller effect on the surface current than the remote improvement of the oceanic circulation, at least in spring.

The EQ-U experiment reproduces nearly the same impact on mean SST and spring cooling (Fig. 11e–f) as EQ-UV, implying that the main driver of the improvement is the zonal wind stress. Consistently, EQ-U equatorial currents are similar to those simulated in EQ-UV (Fig. 14c, d). A realistic zonal wind stress forcing is thus a necessary condition to capture a reasonable spring cooling, consistently with Giordani and Caniaux (2011). They show that one of the main contributors to the equatorial upwelling is the vertical shear of the zonal momentum flux, which is strongly driven by the zonal surface wind stress. Correcting the zonal wind consistently improves this vertical shear and thus the spring equatorial upwelling.

The incorrect representation of surface winds in the coupled simulation might be due either to some intrinsic deficiency of the atmospheric model or to some coupling feedbacks. The AMIP biases are relatively modest (Fig. 8b), especially over the eastern part of the equatorial basin. They are slightly larger in the western tropical Atlantic, particularly for the zonal component. As shown in Moore et al. (1978) and in Busalacchi and Picaut (1983), the wind stress over the western equatorial Atlantic is crucial to drive the ACT, thus AMIP biases could well explain the ACT biases. The EQ-UV-AMIP experiment, where the coupling feedbacks on wind are switched off, allows disentangling the role of the atmospheric biases and coupling feedbacks. In this simulation, mean biases are slightly modified and the spring cooling intensity is slightly increased, particularly in the western equatorial region (Fig. 11g–h). Figure 14f indicates that the ocean equatorial circulation is only partially restored. Wind errors are thus intrinsically present in the atmospheric model. Though modest, they need to be carefully addressed, with the relevant level of precision.

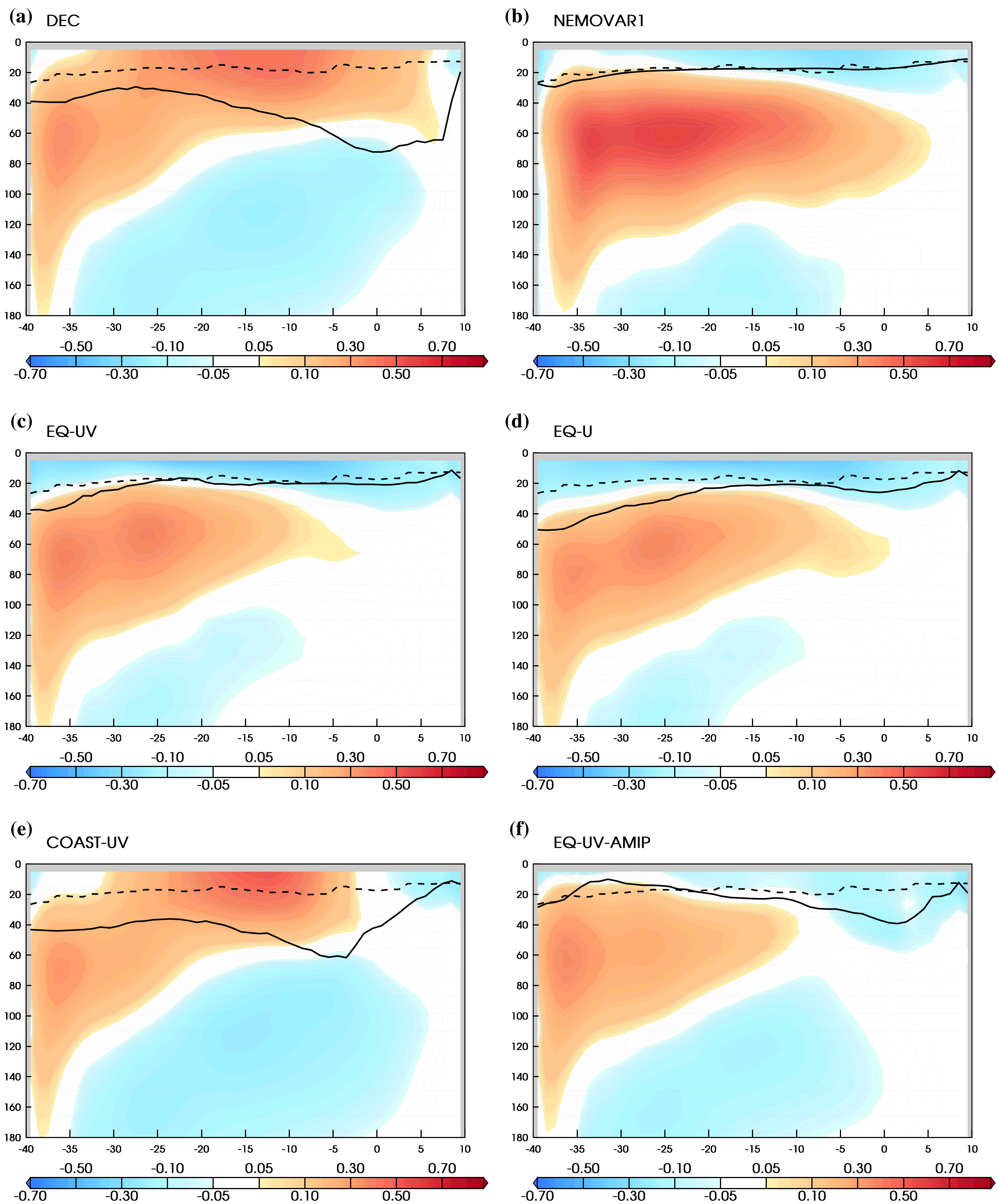
(a) DEC
(b) NEMOVAR1
(c) EQ-UV
(d) EQ-U
(e) COAST-UV
(f) EQ-UV-AMIP
-0.50 -0.10 0.05 0.30 0.70
-0.70 -0.30 -0.05 0.10 0.50

◀ **Fig. 14** Depth-longitude cross-section of zonal currents averaged between 1S–1N in m s^{-1} at the Equator in March–April–May for **a** the decadal experiment, **b** the NEMOVAR1 reanalysis data, **c** EQ-UV, **d** EQ-U, **e** COAST-UV and **f** EQ-UV-AMIP. For all experiments but NEMOVAR1, this is the ensemble mean over the three members started in 1995. The *solid black line* indicates the depth of the turbocline (defined as the depth where the turbulent kinetic energy drops bellow $5.10^{-4} m^2 s^{-1}$) in the respective experiments and the dashed line indicates the depth of the thermocline in the De Boyer-Montégut et al. (2004) observed data set

5 Discussion

The wind nudged experiments emphasized the importance of the surface wind representation in the coupled model to better simulate the ocean circulation, and improve the ACT representation, consistently with the studies of Richter et al. (2012); Wahl et al. (2011) and Huang et al. (2007), who highlight the role of the atmospheric circulation to improve the oceanic representation in the equatorial Atlantic. The improvement of the ACT does not mean a reduced annual mean bias, only an increase of the change in SSTs in spring. The increase of the early spring bias reveals that other terms of the heat budget (surface heat flux or ocean heat transport) are probably misrepresented in the model. The present study indicates that the zonal wind representation in a narrow equatorial band (1.5°S–1.5°N) is crucial. In Wahl et al. (2011), the role of off-equatorial winds is also important, but it does not seem to be the case in CNRM-CM5 (experiment not shown). The meridional component is probably better simulated than the zonal component, so that its correction have a weaker effect even if its forcing is significant. When used according to the AMIP protocol, the CNRM-CM atmospheric model fails to simulate surface winds accurately enough to fully drive the equatorial ocean circulation. The atmospheric model itself requires improvements in the realism of the equatorial zonal wind representation, especially during spring (Fig. 15c), when the ACT develops. In March and April, the zonal wind is nearly positive all along the Equator, while it is negative to the West of 5°W in the ERA-Interim reanalysis (Fig. 15a). Consistently with Grodsky et al. (2012), the ocean-atmospheric coupling induces a positive feedback on the zonal wind bias, reinforcing its westward bias (Fig. 15b).

The impact of atmospheric wind on oceanic turbulent mixing and advection can be diagnosed by the surface Wind Energy Flux, which represents the kinetic energy flux injected into the ocean by the wind stress (Peixoto and Oort 1992; Giordani et al. 2013). The WEF characterises the air-sea energy coupling. In the NEMOVAR1 reanalysis, it is large along the Equator, between 30°W and 0°E (Fig. 16a). In the DEC experiment, the WEF is not active along the Equator and strongly over-estimated north of it, near the African coast (Fig. 16c). Turbulent kinetic energy is generated at the wrong location, picturing erroneous air-sea coupling in CNRM-CM. In the EQ-UV experiment (Fig. 16d), the WEF pattern becomes similar to that in the reanalysis. When calculated using the AMIP simulation surface winds and the NEMOVAR1 surface currents, the WEF realism is improved, but its intensity remains underestimated along the Equator, and close to zero between 10°W and 0°E (Fig. 16b). The WEF underestimate is mainly explained by its zonal component (not shown), which still highlights that the CNRM-CM atmospheric component does not simulate the equatorial zonal wind at the Equator with the appropriate realism. In particular, strong WEF values are limited in their zonal extension along the Equator, emphasizing the importance of atmospheric winds over a relatively small region.

Wahl et al. (2011) showed that correcting the wind impacted the zonal SST gradient, which in turn induces changes in convection and precipitation. In the present sensitivity experiments, no significant effect on African precipitation is observed and the effect on Amazonian precipitation remains weak (not shown). As internal variability of precipitation is large, an ensemble of increased size is probably required to assess this impact. Atmospheric nudging also prevents to rigorously assess it, as it has a direct effect on precipitation, which could interact with SST feedbacks.

If the wind forcing appears to be of primary importance to drive the equatorial ocean circulation and to promote the spring cooling, the annual mean bias is not reduced and even slightly increased in the Guinean Golf. The mixed layer depth is shallower when the wind is corrected, but this tends to increase again the SST all over the year except in early summer. No atmospheric heat flux was shown to be directly responsible for this warm bias here. This suggests that ocean mixing and/or horizontal advection are of primary importance in this region and that the ocean model fails to properly simulate it. This problem has to be investigated more thoroughly in the future and is beyond the scope of the present study. However, the role of barrier layer, as pointed out in Breugem et al. (2008), could be important here in relation with the precipitation bias, which may lead to an over-estimate of the net freshwater flux. Note that the precipitation bias is very weak in AMIP mode, thus this bias is due to coupled feedbacks. Additional experiments would be needed to quantify the role of the freshwater bias on the ocean simulation.

In contrast to the present results with the COAST-UV experiment, Grodsky et al. (2012) found that the wind in the southeastern tropical Atlantic is an important factor driving the northward transport of cool water along the coast. In COAST-UV, this effect is weak. Several reasons can be mentioned: (1) the CNRM-CM atmospheric and

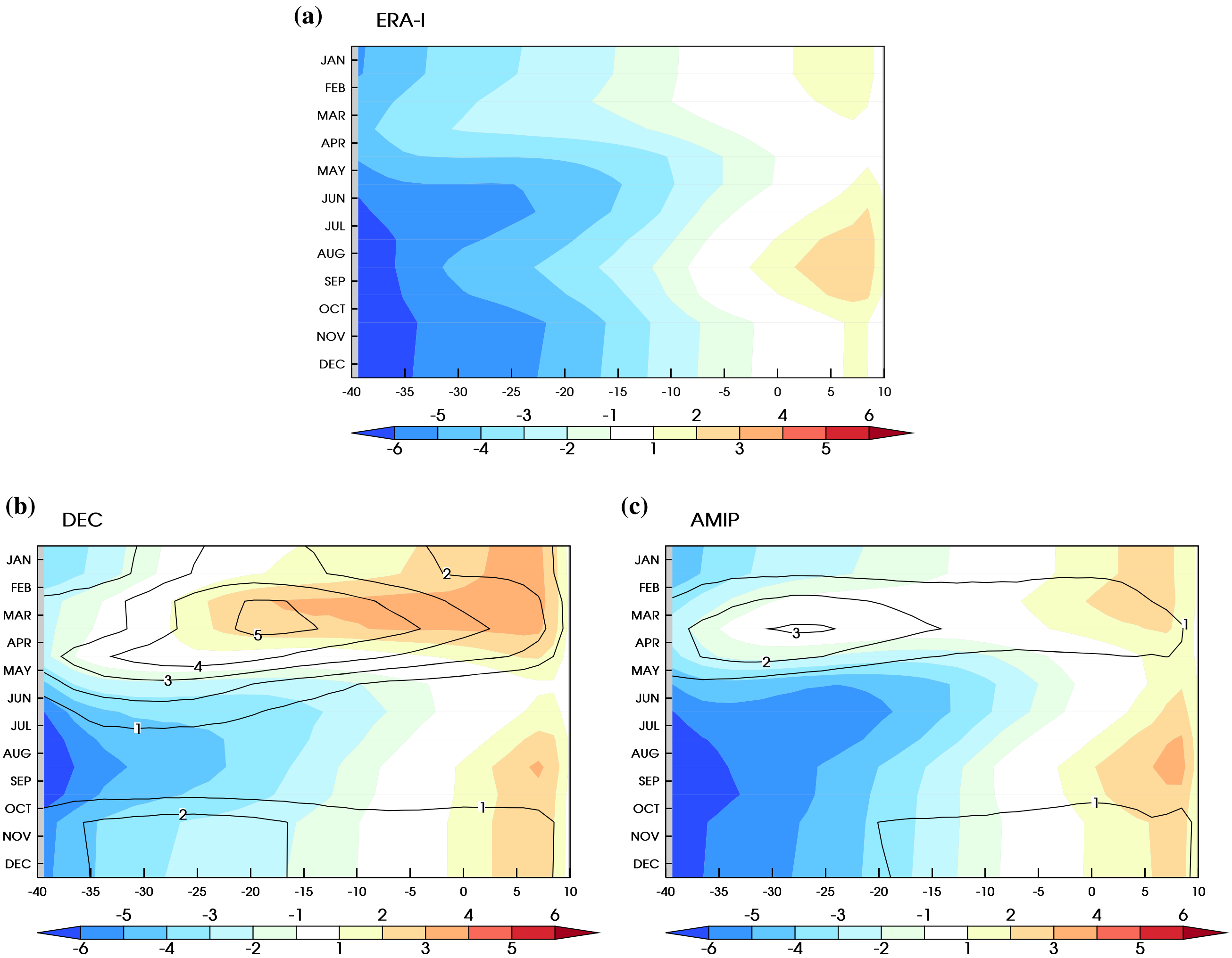

Fig. 15 Hovmoeller diagram of Equatorial surface wind averaged between 1S–1N in m s^{-1} between 40W and 10E in **a** the ERA-Interim data averaged over 1970–1999, **b** the decadal experiment averaged over all start dates and members and **c** the AMIP experiment averaged over 1979–2006. The contour *black line* indicate the difference to the ERA-Interim data

oceanic resolutions are not fine enough to capture these coastal effects, (2) the ERA-Interim wind used for nudging is not realistic enough in the coastal region, and (3) the behaviour described by Grodsky et al. (2012) is model-dependent. The investigation of this difference however remains beyond the scope of the present analysis.

The solar heat flux biases have also been shown to be partly responsible for the annual mean SST bias in the southeastern tropical Atlantic but to have a limited impact on the ACT intensity. In opposite, atmospheric wind biases are related to the main deficiency of CNRM-CM to simulate the spring cooling but induce little change in the SST mean bias locally. As the wind bias mainly impacts on the ocean circulation realism, the question of the feedbacks between the two biases arises. Could both correction further reduce the SST biases and improve the ACT realism? Such a feedback mechanism is suggested by Wahl et al. (2011) and Hu and Huang (2007). It is assessed in CNRM-CM5 using an additional sensitivity experiment ADD, in which both the equatorial wind and the southeastern net solar heat flux are corrected. This experiment is a combination of the EQ-UV and SSC experiments. In ADD (Fig. 16a, b), the SST biases are reduced of the same magnitude as in SSC, with amplification along the coast corresponding to the signal in EQ-UV. No significant feedback on the mean SST bias between the two corrections can be diagnosed (not shown). The decrease in the equatorial spring cooling bias seems also additive, except in the southeastern tropical Atlantic where it is slightly enhanced in ADD. As a result, the feedback between the wind and surface down welling shortwave flux biases is weak. However, in ADD, the ocean–atmosphere couplings are noticeably perturbed, and similar test using an improved model may provide a different response.

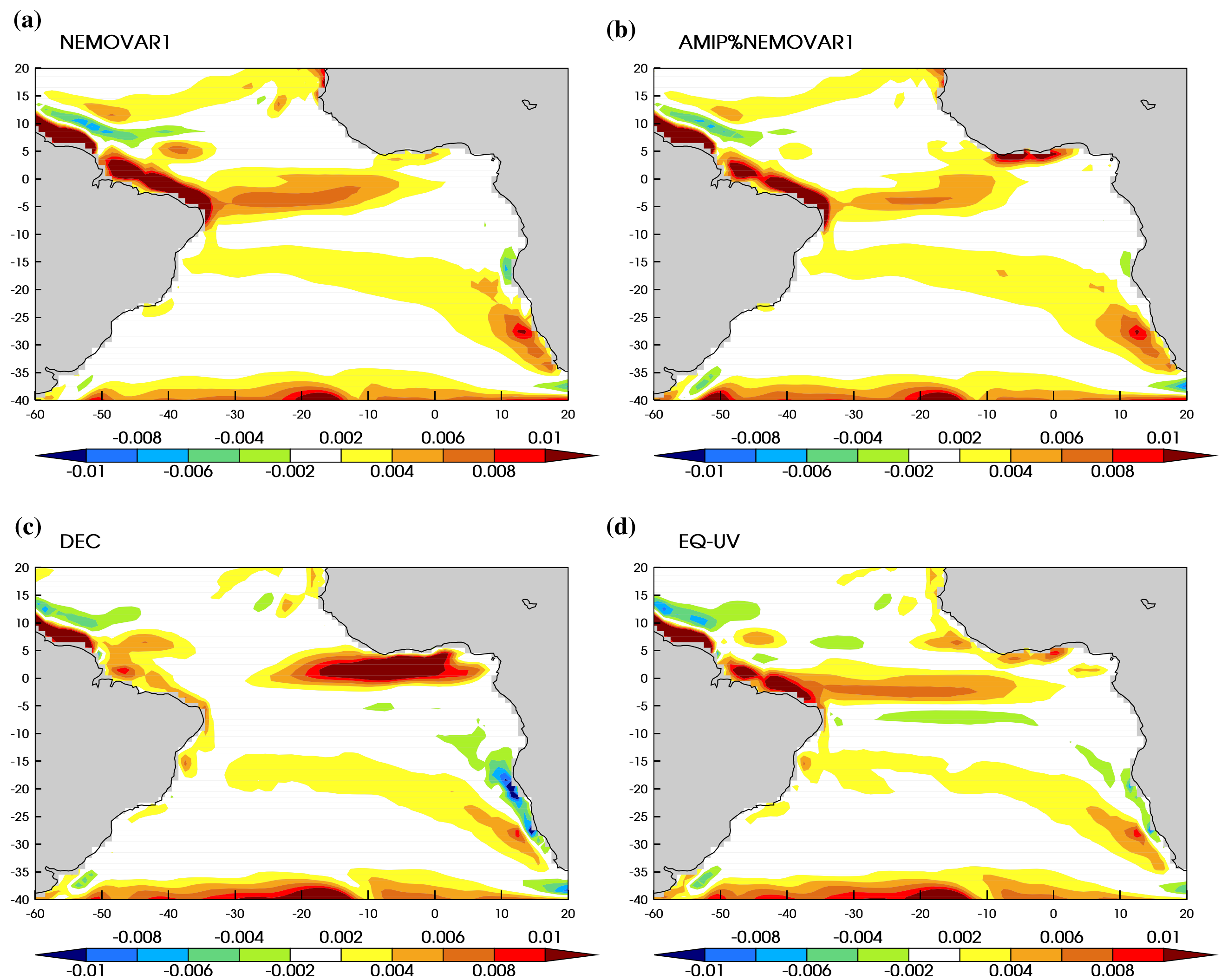

Fig. 16 Wind energy flux in N m^{-1} s^{-1} in MAM **a** for the NEMOVAR1 reanalysis, **b** using the AMIP wind stress and the NEMOVAR1 surface current, **c** for the decadal experiment (DEC) and **d** for the EQ-UV experiment

Finally, the magnitude of the bias reduction compared to the initial bias is quantified (Fig. 17c, d). If the surface wind and surface downwelling shortwave flux were "perfect" (ADD experiment), how much improvement of CNRM-CM could be expected (from the DEC experiment)? The annual mean SST bias is reduced by more than 40 % in the southeastern tropical Atlantic where the solar heat flux is reduced and up to 100 % along the southwestern flank of the correction region. Atmospheric corrections reduce the positive spring cooling bias by more than 40 % all over the ACT region.

Note that in the present experiments, the solar heat flux correction has been uniformly applied over a limited region, so that the correction is not equivalent at each gridpoint. Though refined experiments can be planned, the present protocol point out the bias origins and allows the quantification of their order of magnitude. Atmospheric biases thus explain at least 40 % of the CNRM-CM coupled SST biases. The surface shortwave flux bias is likely to be reduced through the improvement of the SST-radiation-cloud interactions in the atmospheric model. The origin of the surface wind bias deserves further investigation, but might be the footprint of biases in the regional circulation induced by the African and Amazonian convective area (Richter et al. 2012) and/or unrealistic momentum entrainment across the top of the oceanic boundary layer (Zermeño and Zhang 2013).

6 Conclusion

In this study, we have analysed the tropical Atlantic warm SST bias in the CNRM-CM5 model. This warm bias is one of the major weaknesses of state-of-the-art global ocean–

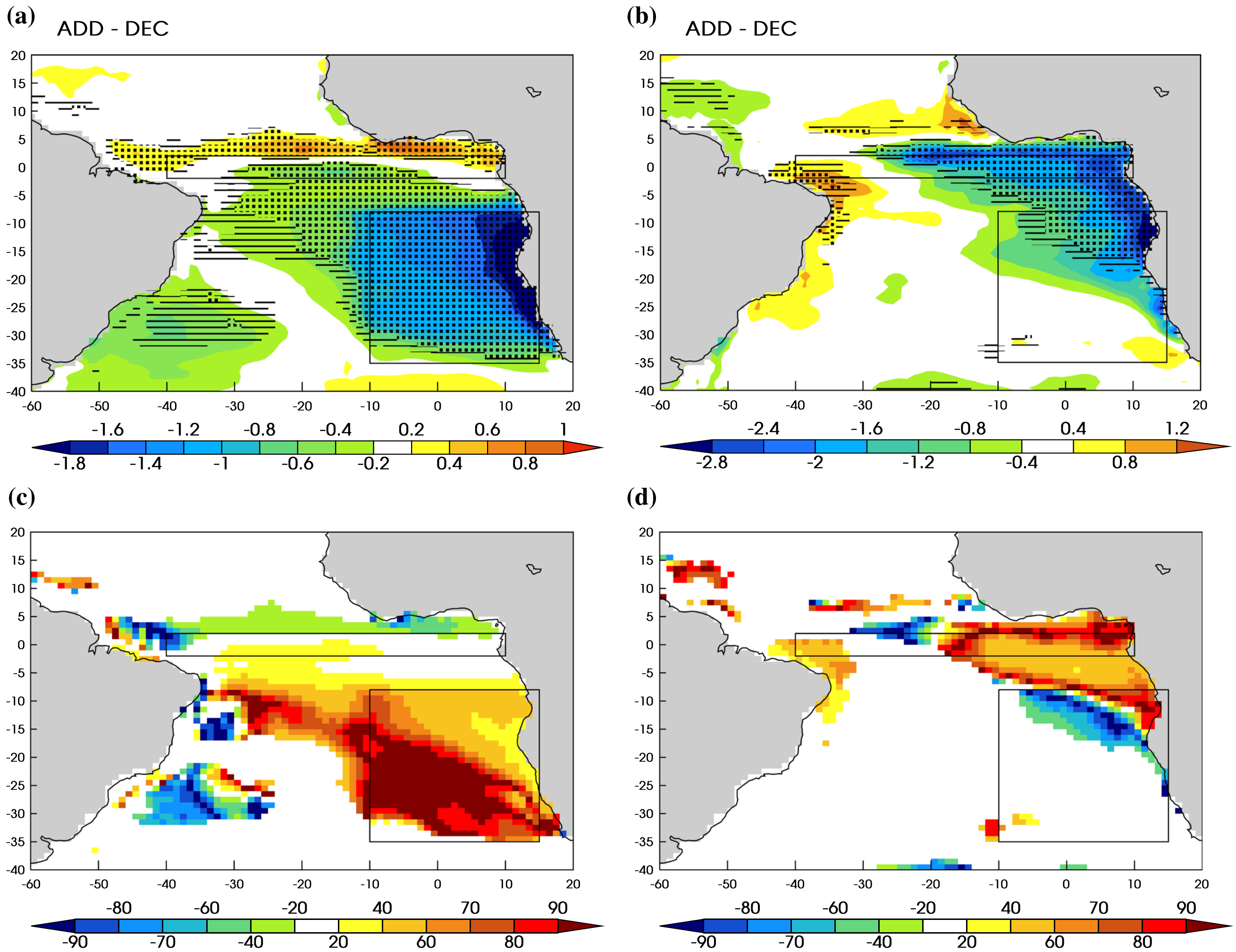

Fig. 17 **a**, **b** Same as Fig. 9 for experiment ADD. **c**, **d** corresponding percentage bias reduction calculated as (1 − abs(bias(ADD)/bias(DEC))×100 where the changes are significant in the corresponding figure of the *upper panel*

atmosphere coupled models that participated to the CMIP5 exercise. It is pointed out that the annual mean SST bias is distinct from the bias in the SST Spring cooling in both the CNRM-CM5 model and the CMIP5 models. The SST Spring cooling bias is maximum along the Equator, whereas the annual mean SST bias is maximum in the southeastern tropical Atlantic. The need to consider two distinct metrics to characterize the tropical Atlantic SST biases is emphasized.

The role of atmospheric biases in initiating the annual mean and spring cooling SST biases has been quantified using several sensitivity experiments. The annual mean SST bias appears within 1 or 2 months when initialising in January, so that short-term (1-year) initialized integrations of CNRM-CM5 provide a useful and light protocol to run sensitivity experiments. Following this approach, partial corrections of the surface wind and/or of the surface net solar heat flux have been applied in CNRM-CM5. The spring wind biases do not settle correctly the ocean equatorial circulation and thus limit the spring equatorial cooling. In contrast, the surface net solar heat flux overestimate impacts the southeastern Atlantic SSTs all year long. The warm SST bias originates from two different patterns, occurring at two different timescales (seasonal and annual mean). On the one hand, the solar heat flux correction in the southeastern tropical Atlantic locally reduces the SST bias, with a weak effect over the Equator in summer. On the other hand, the wind stress correction mainly impacts the spring cooling at the local scale, with a small remote effect of equatorial winds on the SST bias along the eastern African coast. As highlighted in several studies (Huang et al. 2007; Lubbecke et al. 2010; Grodsky et al. 2012), two regions, which strongly interact, have to be considered. This study mainly stresses the role of the wind in driving the ocean circulation and in allowing the spring cooling which is important to amplify the annual cycle amplitude in SSTs, whereas the solar flux has an impact on the annual mean bias.

The role of the surface zonal wind has been particularly emphasized. However, in contrast to the Wahl et al. (2011) study, the role of off-equatorial wind is less clear in CNRM-CM5. The WEF diagnostic provided some physical basis to understand its importance to drive the equatorial upwelling, especially in the western region. A high-level realism of the atmospheric large-scale circulation appears crucial, at least in CNRM-CM5, since a shift of a few degrees in the position of large-scale features may results in inappropriate zonal wind at the Equator as analyzed in the AMIP-type simulation. Richter et al. (2012) showed that by promoting the convection over the equatorial South America, trade winds were better simulated and SST biases consequently reduced. Wind biases are thus likely a local and/or remote response to deficiencies in the atmospheric model physics.

As in Wahl et al. (2011), the coupling largely amplifies the biases. Nearly half of the bias is attributable to ocean–atmosphere feedbacks. This study mainly confirms former results with another model but using a different correction technique for the winds (the nudging), which have the advantage of impacting consistently the surface heat fluxes, and a different experiment protocol. As in Wahl et al. (2011) the respective role of the winds and the solar fluxes in yielding warm SST biases are quantified. This study confirms most of the results highlighted in the Wahl et al. (2011) study done with the Kiel Climate Model, except the importance of off-equatorial winds.

The "partial correction" methodology appears as a powerful tool to quantify different sources of errors in models. In the present paper, it also allows to better assess the ability of the oceanic model in reproducing the observed climate, particularly SSTs, in a less constrained framework than in ocean forced simulations. Applying such corrections, first-order flaws, such as the ocean circulation, are corrected and second-order flaws, more intrinsic to the ocean model, appear more evidently. Oceanic processes at work in the region can thus be analysed more in depth and sensitivity experiments to ocean parameterisations/processes can be proposed. In particular, in the Guinean Gulf, the CNRM-CM5 ocean component experienced difficulties not attributable to atmospheric flaws. This deficiency may be disentangled in the corrected-wind simulations analysing the sensitivity to the vertical mixing parameterisation.

The present analysis focussed on the mean seasonal cycle. Interestingly, the proposed framework can be used to quantify the role of partial corrections at specific location in the simulated interannual variability of the tropical Atlantic.

Acknowledgments The authors wish to thank C. Cassou and E. Sanchez for providing the CNRM-CM5 decadal simulations and for helpful discussions. Thanks to the two anonymous reviewers for their helpful comments. The authors also thank the global ocean heat flux and evaporation products that were provided by the WHOI OAFlux project (http://oaflux.whoi.edu) funded by the NOAA Climate Observations and Monitoring (COM) program.

References

Balmaseda M, Mogensen K, Molteni F, Weaver A (2010) The NEMOVAR-COMBINE ocean re-analysis. COMBINE Technical report No. 1. Available from http://www.combine-project.eu/Technical-Reports.1668.0.html

Barnier B et al (1995) Thermal forcing for a global ocean circulation model using a three-year climatology of ECMWF analyses. J. Mar. Sys. 6:363–380

Batté L, Déqué M (2011) Seasonal predictions of precipitation over Africa using coupled ocean-atmosphere general circulation models: skill of the ENSEMBLES project multimodel ensemble forecasts. Tellus-A 63:283–299. doi:10.1111/j.1600-0870.2010.00493.x

Belamari S (2005) Report on uncertainty estimates of an optimal bulk formulation for surface turbulent fluxes. MERSEA IP Deliverable, D.4.1.2, 29

Bourlès B, Lumpkin R, McPhaden MJ, Hernandez F, Nobre P, Campos E, Yu L, Planton S, Busalacchi AJ, Moura AD, Servain J, Trotte J (2008) The PIRATA program: history, accomplishments, and future directions. Bull Am Meteorol Soc 89(8):1. doi:10.1175/2008BAMS2462.1

Breugem W-P, Chang P, Jang CJ, Mignot J, Hazeleger W (2008) Barrier layers and tropical Atlantic SST biases in coupled GCMs. Tellus A 60:885–897. doi:10.1111/j.1600-0870.2008.00343.x

Busalacchi AJ, Picaut J (1983) Seasonal variability from a model of the tropical Atlantic ocean. J Phys Oceanogr 13:1564–1588

Caniaux G, Giordani H, Redelsperger JL, Guichard F, Key E, Wade M (2011) Coupling between the Atlantic cold tongue and the West African monsoon in boreal spring and summer. J Geophys Res 116:C04003. doi:10.1029/2010JC006570

Césana G, Chepfer H (2012) How well do climate models simulate cloud vertical structure? A comparison between CALIPSO-GOCCP satellite observations and CMIP5 models. Geophys. Res. Letters 39:L20803. doi:10.1029/2012GL053153

Chang CY, Carton JA, Grodsky SA, Nigam S (2007) Seasonal climate of the tropical Atlantic sector in the NCAR Community Climate System Model 3: error structure and probable causes of errors. J Clim 20:1053–1070

De Boyer-Montégut C, Madec G, Fisher AS, Lazar A, Iudicone D (2004) Mixed layer depth over the global ocean: an examination of profile data and a profile-based climatology. J Geophys Res 109:C12003. doi:10.1029/2004JC002378

Dee DP et al (2011) The ERA-Interim reanalysis: configuration and performance of the data assimilation system. Quat. J. of Roy. Met. Soc. 137:553–597. doi:10.1002/qj.828

DeSzoeke SP, Fairall CW, Wolfe DE, Bariteau L, Zuidema P (2010) Surface flux observations on the southeastern tropical Pacific Ocean and attribution of SST errors in coupled ocean–atmosphere models. J. Climate 23:4152–4174

Fennig K, Bakan S, Grassl H, Klepp C-P, Schulz J (2006) Hamburg Ocean atmosphere parameters and fluxes from satellite data—HOAPS II—monthly mean., electronic publication, WDCC, doi:10.1594/WDCC/HOAPS2_MONTHLY

Foltz GR, Grodsky SA, Carton JA, McPhaden MJ (2003) Seasonal mixed layer heat budget of the tropical Atlantic Ocean. J Geophys Res 108:3146. doi:10.1029/2002JC001584

Giordani H, Caniaux G (2011) Diagnosing vertical motion in the equatorial Atlantic. Ocean Dyn 61(12):1995–2018

Giordani H, Caniaux G, Voldoire A (2013) Intraseasonal mixed layer heat budget in the equatorial Atlantic during the cold tongue development in 2006. J. of Geophys. Res. Oceans 118:1–22. doi:10.1029/2012JC008280

Grodsky SA, Carton JA, Nigam S, Okumura YM (2012) Tropical Atlantic biases in CCSM4. J Clim 25:3684–3701. doi:10.1175/JCLI-D-11-00315.1

Guilyardi E, Cai WJ, Collins M, Fedorov A, Jin FF, Kumar A, Sun DZ, Wittenberg A (2012) New strategies for evaluating ENSO processes in climate models. Bull. Ame. Met. Soc. 93:235–238

Hu Z, Huang B (2007) Physical processes associated with the tropical Atlantic SST gradient during the anomalous evolution in the southeastern ocean. J Clim 20:3366–3378

Hu ZZ, Huang B, Hou YT, Wang W, Yang F, Stan C, Schneider EK (2011) Sensitivity of tropical climate low-level clouds in the NCEP climate forecast system. Clim Dyn 36:1795–1811. doi:10.1007/s00382-010-0797-z

Huang B, Hu ZZ, Jha B (2007) Evolution of model systematic errors in the tropical Atlantic basin from coupled climate hindcasts. Clim Dyn 28:661–682. doi:10.1007/S00382-006-0223-8

Intergovernmental Panel on Cliamte Change (2007) Climate change 2007: the physical science basis. In: Solomon S (ed) Contribution of working group I to the fourth assessment report of the intergovernmental panel on climate change. Cambridge University Press, Cambridge

Joly M, Voldoire A (2010) Role of the Gulf of Guinea in the interannual variability of the West African monsoon: what do we learn from CMIP3 coupled simulations ? Int J Clim 30(12):1843–1856. doi:10.1002/joc.2026

Klein et al (2013) Are climate model simulations of clouds improving? An evaluation using the ISCCP simulator. J Geophys Res Atm 118:1329–1342. doi:10.1002/jgrd.50141

Lin J-L (2007) The double-ITCZ problem in IPCC AR4 coupled GCMs: ocean–atmosphere feedback analysis. J Clim 20:4497–4525

Lubbecke JF, Boning CW, Keenlyside NS, Xie SP (2010) On the connection between Benguela and equatorial Atlantic niños and the role of the south Atlantic anticyclone. J Geophys Res 115:C09015. doi:10.1029/2009JC005964

Moore D, Hisard P, McCreary JP, Merlo J, O'Brien JJ, Picaut J, Vestraete JM, Wunsch C (1978) Equatorial adjustment in th eastern Atlantic. Geophys Res Lett 5:637–640

Peixoto JP and Oort AH (1992) Physics of Climate, American Institute of Physics Ed

Rayner NA, Parker DE, Horton EB, Folland CK, Alexander LV, Rowell DP, Kent EC, Kaplan A (2003) Global analyses of sea surface temperature, sea ice, and night marine air temperature since the late nineteenth century. J Geophys Res 108(D14):4407. doi:10.1029/2002JD002670

Richter I, Xie S (2008) On the origin of equatorial Atlantic biases in coupled general circulation models. Clim Dyn 31:587–598. doi:10.1007/s00382-008-0364-z

Richter I, Xie S-P, Wittenberg AT, Masumoto Y (2012) Tropical Atlantic biases and their relation to surface wind stress and terrestrial precipitation. Clim Dyn 38:985–1001. doi:10.1007/s00382-011-1038-9

Richter I, Xie S-P, Behera SK, Doi T, Masumoto Y (2013) Equatorial Atlantic variability and its relation to mean state biases in CMIP5, Clim. Dyn., doi:10.1007/s00382-012-1624-5, online

Roehrig R, Bouniol D, Guichard F, Hourdin F and Redelsperger J-L (2013) The present and future of the West African monsoon: a process-oriented assessment of CMIP5 simulations along the AMMA transect, J. of Climate, under revision

Rossow WB, Walker AW, Beuschel DE and Roiter MD (1996) International Satellite Cloud Climatology Project (ISCCP) Documentation of New Cloud Datasets. WMO/TD-No. 737, World Meteorological Organization, 115 pp

Seo H, Jochum M, Murtugudde R, Miller AJ (2006) Effect of ocean mesoscale variability on the mean state of tropical Atlantic climate. Geophys Res Lett 33:L09606. doi:10.1029/2005GL025651

Su et al (2013) Diagnosis of regime-dependent cloud simulation errors in CMIP5 models using "A-Train" satellite observations and reanalysis data. J Geophys Res Atm 118:2762–2780. doi:10.1029/2012JD018575

Taylor KE, Stouffer RJ, Meehl GA (2012) An overview of CMIP5 and the experiment design. Bull Am Meteor Soc 93:485–498. doi:10.1175/BAMS-D-11-00094

Toniazzo T and Woolnough S (2013) Development of warm SST errors in the southeastern tropical Atlantic in CMIP5 decadal hindcasts, Clim Dyn, doi:10.1007/s00382-013-1691-2

Voldoire A, Sanchez-Gomez AE, Salas y Mélia D, Decharme B, Cassou C, Sénési S, Valcke S, Beau I, Alias A, Chevallier M, Déqué M, Deshayes J, Douville H, Fernandez E, Madec G, Maisonnave E, Moine M-P, Planton S, Saint-Martin D, Szopa S, Tyteca S, Alkama R, Belamari S, Braun A, Coquart L, Chauvin F (2013) The CNRM-CM5.1 global climate model: description and basic evaluation. Clim Dyn. doi:10.1007/s00382-011-1259-y

Wade M, Caniaux G, DuPenhoat Y (2011) Variability of the mixed layer heat budget in the Eastern Equatorial Atlantic during 2005-2007 as inferred using Argo floats. J Geophys Res 116:C08006. doi:10.1029/2010JC006683

Wahl S, Latif M, Park W, Keenlyside N (2011) On the tropical Atlantic SST warm bias in the Kiel climate model. Clim Dyn 36:891–906

Weill A, Eymard L, Caniaux G, Hauser D, Planton S, Dupuis H, Brut A, Guerin C, Nacass P, Butet A, Cloché S, Pedreros R, Durand P, Bourras D, Giordani H, Lachaud G, Bouhours G (2003) Toward a better determination of turbulent air-sea fluxes from several experiments. J Clim 16:600–618

Yu L, Jin X, and Weller RA (2008) Multidecade Global Flux Datasets from the Objectively Analyzed Air-sea Fluxes (OAFlux) Project: Latent and sensible heat fluxes, ocean evaporation, and related surface meteorological variables. Woods Hole Oceanographic Institution, OAFlux Project Technical Report. OA-2008-01, 64 pp. Woods Hole. Massachusetts

Zebiac SE (1993) Air-sea interaction in the equatorial Atlantic region. J Clim 6:1567–1586

Zermeño D, Zhang C (2013) Possible root causes of the surface westerly bias over the equatorial Atlantic in Atmospheric Global Climate Model. J Clim. doi:10.1175/JCLI-D-12-00226.1

Zhang W, Jin F–F (2012) Improvements in the CMIP5 simulations of ENSO-SSTA meridional width. Geophys Res Lett 39:L23704. doi:10.1029/2012GL053588

Zhang T, Stackhouse PW, Gupta SK, Cox SJ, Mikovitz JC, Hinkelman LM (2013) The validation of the GEWEX SRB surface shortwave flux data products using BSRN measurements: a systematic quality control, production and application approach. J Quant Spectrosc Radiat Transf. doi:10.1016/j.jqsrt.2012.10.004

Zheng Y, Shinoda T, Lin J-L, Kiladis GN (2011) Sea surface temperature biases under the stratus cloud deck in the southeast Pacific Ocean in 19 IPCC AR4 coupled general circulation models. J Clim 24:4139–4164